

EUROPEAN LABORATORY FOR PARTICLE PHYSICS

CERN SL Division

CERN LIBRARIES, GENEVA

CERN SL/94-71 (BI)



CERN-SL-94-71

Accurate Determination of the LEP Beam Energy by Resonant Depolarization

L. Arnaudon, R. Assmann¹, A. Blondel², B. Dehning,
P. Grosse-Wiesmann, R. Jacobsen, M. Jonker, J.P. Koutchouk,
J. Miles, R. Olsen, M. Placidi, R. Schmidt, J. Wenninger

Abstract

To improve the measurements of the Z boson mass and resonance width, the 1993 Large Electron Positron Collider (LEP) run was devoted to a three point beam energy scan, with one point close to the peak of the Z resonance and two points roughly 880 MeV below and above the peak. Operational energy calibration by resonant depolarization was successfully commissioned for all three beam energies. 24 energy calibrations were performed at the end of physics fills. The accuracy of each calibration is better than 1 MeV. About one third of the total integrated luminosity was recorded in calibrated fills below and above the resonance and a regular tracking of the beam energies throughout the scan was possible. The evolution of the beam energies in the course of the year showed a large variation of up to 20 MeV. Results from the energy calibrations will be presented and possible explanations for the changes of the beam energy during the year will be described.

Geneva, Switzerland

1 August 1994

¹Max-Planck-Institut für Physik, Werner-Heisenberg-Institut, München, Germany

²Ecole Polytechnique, Paris, France

Contents

1	Introduction	3
2	Principle of energy calibration by resonant depolarization	3
3	Energy calibration accuracy	7
3.1	Electron mass and magnetic moment anomaly	7
3.2	Revolution frequency	7
3.3	Frequency of the RF-magnet	7
3.4	Width of the excited spin resonance	7
3.5	Interference between depolarizing resonances	9
3.6	Spin tune shifts due to longitudinal magnetic fields	9
3.7	Spin tune shifts due to radial magnetic fields	11
3.8	Effects of electrostatic fields	11
3.9	Effects of quadratic non-linearities	11
3.10	Summary on the calibration accuracy	13
4	LEP settings for beam energy calibration	13
4.1	Effects of LEP settings on beam energy	14
4.1.1	Pretzel orbits	14
4.1.2	Betatron tunes	14
4.1.3	Low beta optics	15
4.1.4	Local magnetic bumps	15
5	Models of energy variations and corrections	15
5.1	Magnetic field measurements	15
5.2	Momentum compaction factor	16
5.3	Terrestrial tides	16
5.4	Magnet temperature	18
5.5	QFQD compensation loop	21
5.6	Energy calibration reproducibility and correction quality	22
6	Positron beam energy	24
7	Beam energy calibration results in 1993	25
8	Conclusions	32
9	Acknowledgments	32
A	Appendix : Magnetic field reference	35
B	Appendix : Calibrated fill energies	37

1 Introduction

Between 1990 and 1992 extensive studies were performed at LEP to establish transversely polarized beams and to implement energy calibration by resonant depolarization [1, 2, 3]. As a result the systematic error on the mass of the Z boson due to the knowledge of the absolute energy scale of LEP was reduced to 6 MeV for the 1991 LEP energy scan [4, 5]. Since by the end of 1992 it was possible to envisage a continuous monitoring of the beam energy using resonant depolarization, the 1993 LEP run was devoted to a 3 point energy scan to improve the measurements of the Z mass and resonance width, with a significant reduction of the systematic errors due to a better knowledge of the LEP beam energy compared to the 1991 LEP energy scan.

Improvements on the LEP polarimeter [6, 7, 8], the vertical alignment of the quadrupoles [9] and the beam orbit monitors [10, 11] as well as the successful implementation of deterministic Harmonic Spin Matching [12] allowed to establish transverse polarization on all three energy points for the 1993 scan. Transversely polarized beams were obtained at the end of physics fills thanks to the spin compensation of the experimental solenoids [13] and an improved understanding of depolarizing effects. The procedures to establish polarized beams for energy calibration in LEP are published elsewhere [8].

During the 1993 energy scan which lasted from July to November, 24 calibrations were successfully performed on the electron beams at the end of physics fills, using approximately 5% of the total running time. Systematic effects of the spin dynamics and of the beam energy variations were studied in parallel to energy calibration. While usually the positron beam was dumped for the calibrations, two vertically separated beams were kept during the last week. A first test measurement of the positron energy was obtained.

We report here on the energy calibration procedure and its accuracy, the measurement of parameters that affect the beam energy and the evolution of the beam energy during the year 1993.

2 Principle of energy calibration by resonant depolarization

Transverse beam polarization in LEP opens the possibility for accurate measurements of the average beam energy. The attainable precision is more than one order of magnitude better than that provided by other existing methods [5]. We will first describe the principle of energy calibration by resonant depolarization.

The motion of the spin vector \vec{S} of a relativistic electron in electromagnetic fields \vec{E} and \vec{B} is described by the Thomas-BMT equation [14] :

$$(1) \quad \frac{d\vec{S}}{dt} = \vec{\Omega}_{\text{BMT}} \times \vec{S}$$

$$(2) \quad \vec{\Omega}_{\text{BMT}} = -\frac{e}{\gamma m} \left[(1 + a\gamma) \vec{B}_{\perp} + (1 + a) \vec{B}_{\parallel} - \left(a\gamma + \frac{\gamma}{1 + \gamma} \right) \vec{\beta} \times \frac{\vec{E}}{c} \right]$$

where \vec{B}_{\perp} and \vec{B}_{\parallel} are the components of the magnetic field which are transverse and parallel with respect to the particle's velocity $\vec{\beta}c$. e is the charge, m the mass, a the magnetic moment anomaly and γ the Lorentz factor of the electron.

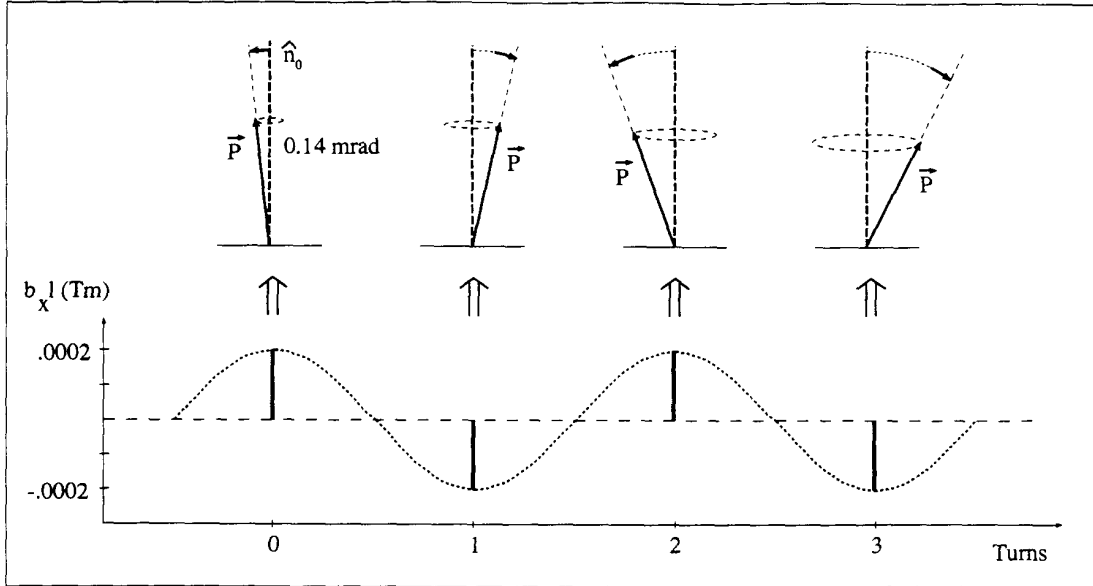


Figure 1: Resonance condition between the nominal spin precession with $[\nu] = 0.5$ and the radial perturbation $\int b_x l$ from the RF-magnet. In an ideal storage ring the polarization vector is initially along the vertical direction. After being tilted \vec{P} precesses with ν about its initial direction. If the perturbation is in phase with the nominal spin precession (in this example $f_{dep} = 0.5 \cdot f_{rev}$) the polarization vector is resonantly rotated away from the vertical direction.

The strongest magnetic fields in a storage ring arise from the dipole bending magnets, which produce vertical fields B_y and maintain the particles on circular orbits. The precession frequency of the particles in the storage ring is given by the cyclotron frequency $\Omega_c = -(e/\gamma m)B_y$. The comparison of Ω_c with the spin precession frequency Ω_{BMT} shows that the spin vector of a particle will precess $a\gamma$ times for one revolution in the storage ring, where the term $a\gamma$ is called the *spin tune*. Its average value ν for all electrons is directly proportional to the average beam energy E [15] :

$$(3) \quad \nu = a\gamma = \frac{aE}{mc^2} = \frac{E[\text{MeV}]}{440.6486(1)[\text{MeV}]}$$

This relation is exact only for ideal storage rings. Its limitations due to imperfections will be discussed later. Throughout this report, if not otherwise stated, all energies are understood to be beam energies and not center-of-mass energies at the interaction points.

In an e^+e^- storage ring with purely vertical magnetic fields the vertical component of the spin vectors is conserved. The ensemble average of all spin vectors is defined as the polarization vector \vec{P} . Due to the Sokolov-Ternov effect vertical polarization can build up to a maximum of 92.4% [16]. Any radial magnetic field reduces the equilibrium degree of polarization and perturbs the spin precession.

An oscillating radial field from an RF-magnet is used for the resonant measurement of the spin precession frequency at LEP. In standard conditions a radial field strength $\int b_x l = 2 \cdot 10^{-4}$ Tm is used to rotate the spin by 140 μ rad about the radial direction. The deflection of the particle trajectories is ν times smaller. If the perturbation from the RF-magnet is in phase with the spin precession, the spin rotations about the radial direction add up coherently

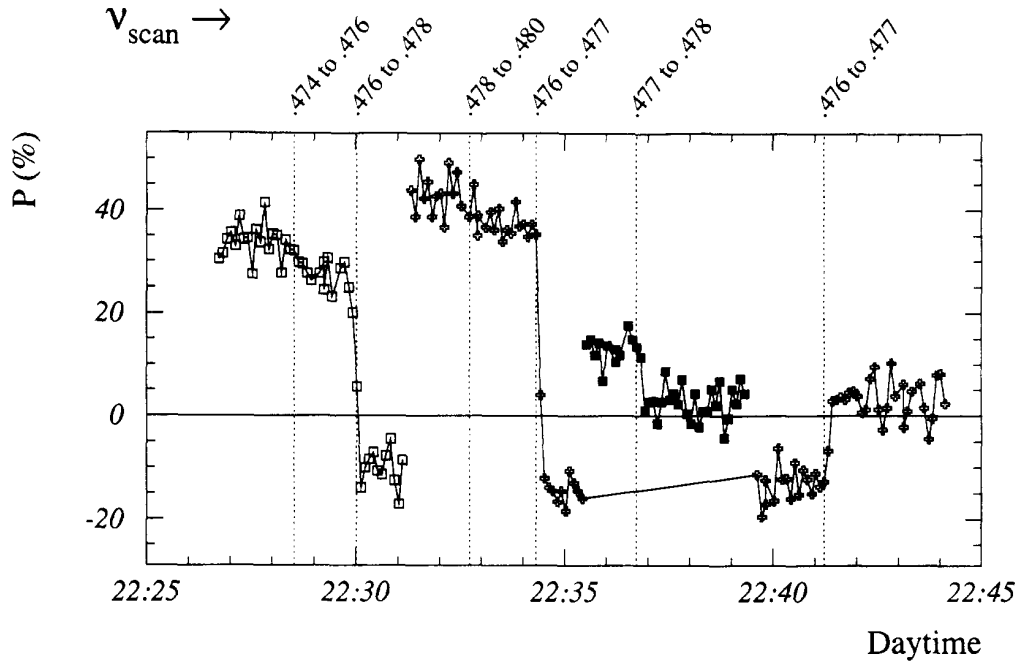


Figure 2: Example of energy calibration by resonant depolarization. Several bunches are used to measure the non-integer part of the spin tune. Frequency scans with the depolarizer are indicated with dotted lines. The frequency limits are indicated on top of the picture for each scan in units of spin tune. The observed depolarizations locate the fractional spin tune close to 0.477. Partial spin flips to negative polarization were observed and checked by flipping them again.

from turn to turn. About 10^4 turns (≈ 1 second) are needed to turn the polarization vector into the horizontal plane, or twice as much to flip its direction. Due to stochastic synchrotron radiation in e^+e^- storage rings, the horizontal component of the polarization vector is unstable and the beam polarization can only partially be flipped. The RF-magnet field oscillating at a frequency f_{dep} is in resonance with the spin precession if :

$$(4) \quad f_{\text{dep}} = (k \pm [\nu]) \cdot f_{\text{rev}}$$

where f_{rev} is the revolution frequency of the particles ($f_{\text{rev}} = 11.25$ kHz at LEP) and k is an integer. $[\nu]$ denotes the non-integer part of the spin tune. Its integer part n is determined from the setting of the bending field. The frequencies f_{dep} used at LEP correspond to the cases $k = 0$ ($f_{\text{dep}} = [\nu] \cdot f_{\text{rev}}$) or $k = +1$ ($f_{\text{dep}} = (1 - [\nu]) \cdot f_{\text{rev}}$). The resonance condition is illustrated for $[\nu] = 0.5$ in figure 1. The frequency f_{dep} is varied until a depolarization is observed. The spin tune $\nu = [\nu] + n$ can then be calculated with equation 4 from the measured f_{dep} and the average beam energy E is obtained from equation 3. This method is often referred to as *energy calibration by resonant depolarization* and has been used extensively for accurate beam energy calibrations and measurements of particle masses [17, 18, 19, 20, 21, 22]. It is important to notice that it is the precession frequency of the polarization vector over one turn which is determined and not the beam energy of individual particles at the location of the RF-magnet. Because the polarization vector is the ensemble average over all spin vectors, the measured beam

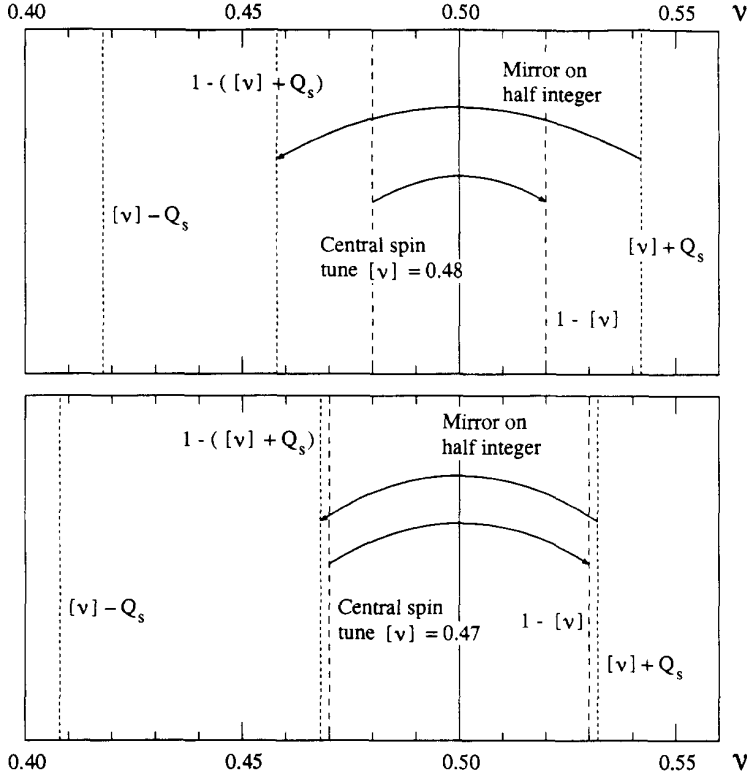


Figure 3: The locations of the synchrotron satellites and the mirror resonances are indicated for two different central spin tunes in the case $Q_s = 0.0625$. Depending on the value of $[\nu]$, Q_s , sideband resonances can appear close to the main resonance. The beam energy can however always be determined uniquely by changing the beam energy and the synchrotron tune.

energy is to a very good approximation independent of betatron and synchrotron oscillations of the individual particles and is not limited in accuracy by the LEP beam energy spread (35 MeV at 45 GeV). Local energy variations like the energy sawtooth modify the spin phase advance. They do not however bias the measured beam energy which is determined from the total spin phase advance over one complete turn.

Experimentally the frequency of the RF-magnet field is slowly varied with time over a given range. The width Δf_{dep} of the frequency “scan” determines in practice the resolution $\Delta \nu_{scan}$ of the spin tune measurement. For standard calibrations $\Delta \nu_{scan}$ could be set to 0.002 which corresponds to $\Delta f_{dep} = 22.2$ Hz and to an accuracy on the energy of $\Delta E_{scan} = 0.88$ MeV. Since the spin tune is not localized inside the frequency scan, the RMS error on ν is given by $\sigma_\nu = \Delta \nu_{scan} / \sqrt{12}$. On some occasions a resolution of $\Delta \nu_{scan} = 0.0005$ was achieved. Figure 2 shows an example of energy calibration where the fractional spin tune is located close to 0.477. A single bunch can be depolarized selectively leaving the polarization of all other bunches unchanged. Several partial spin flips are observed on different bunches.

Two additional measurements are required to uniquely determine the beam energy because a single energy calibration cannot resolve all ambiguities. A measured non-integer part of the spin tune $[\nu]$ is compatible with a mirrored spin tune of $1 - [\nu]$. To solve this *mirror ambiguity* the beam energy is varied and the corresponding change of f_{dep} is measured. To avoid modifying the magnetic set up the beam energy is varied by changing the RF frequency. Depolarization can also occur on synchrotron satellites which appear at spin tunes of $\nu_{side} = \nu \pm Q_s$. The main resonance ν can be separated from the satellites ν_{side} because it is not shifted by a change of the synchrotron tune Q_s . The locations of synchrotron satellites and mirror resonances are shown in figure 3 for two different spin tunes ν .

3 Energy calibration accuracy

We now discuss the limitations and systematic errors of energy calibration by resonant depolarization for LEP.

3.1 Electron mass and magnetic moment anomaly

The measurement of the electron mass [15] $m = 0.51099906(15)$ MeV sets a fundamental limit on the accuracy of the method. This limit corresponds to a relative error of $\Delta E/E = 3 \cdot 10^{-7}$. The uncertainty on the electron magnetic moment anomaly [15] $a = 1.159652193(10) \cdot 10^{-3}$ is small enough that it can be neglected.

3.2 Revolution frequency

To convert the measured spin precession frequency into a spin tune the revolution frequency f_{rev} of the particles must be known. The uncertainty in f_{rev} introduces a relative error $\Delta E/E = 10^{-10}$ which can be neglected.

3.3 Frequency of the RF-magnet

The frequency f_{dep} of the RF-magnet is produced with a synthesized function generator. According to the instrument specifications f_{dep} is generated with an accuracy of $25 \cdot 10^{-3}$ Hz. Since the spin precession frequency is of the order of 1.1 MHz this leads to an uncertainty of $\Delta E/E = 2 \cdot 10^{-8}$. Experimentally the setting of the frequency was verified with an accuracy of 2 Hz corresponding to $\Delta E/E = 2 \cdot 10^{-6}$.

3.4 Width of the excited spin resonance

The perturbation from the RF-magnet can be considered as an artificial spin resonance excited at a known location in spin tune. If the spin tune of the particles is inside the width of this spin resonance the polarization vector is rotated and the polarization is destroyed or partially flipped. The width ϵ of the excited spin resonance depends on the strength of the RF-magnet and on the frequency change of the RF-magnet field with time, which can be expressed in spin tune as $\Delta\nu_{\text{scan}}/\Delta t$. ϵ was explicitly measured with a reduced bin width $\Delta\nu_{\text{scan}}$ of 0.0005 in spin tune. The standard strength of the RF-magnet ($2 \cdot 10^{-4}$ Tm) was used and the change in polarization $P_{\text{final}}/P_{\text{initial}}$ was measured as a function of spin tune. Two different cases for the slope of spin tune change with time $\Delta\nu_{\text{scan}}/\Delta t$ were considered.

Case (a) in figure 4 was measured with the same parameters that are used for a standard energy calibration. The FWHM of the resonance is 0.2 MeV. This small width is especially remarkable when it is compared to the beam energy spread of about 35 MeV.

Case (b) in figure 4 was measured with a slope $\Delta\nu_{\text{scan}}/\Delta t$ 4 times smaller than case (a). The perturbation from the RF-magnet was in phase with the precessing spin vectors for a longer time than for case (a). This leads to a stronger excitation of the spin resonance whose FWHM increases to 0.8 MeV.

From $\Delta\nu_{\text{scan}}/\Delta t$ and the measured width ϵ of the excited spin resonance the change of polarization $P_{\text{final}}/P_{\text{initial}}$ has been calculated from a formula obtained by Froissart and Stora [23]. Their calculation is only valid for a single particle without synchrotron radiation. In a simple approach we use it for electrons by adding a term $e^{-T/\tau_{\text{decoh}}}$, assuming that the effects of

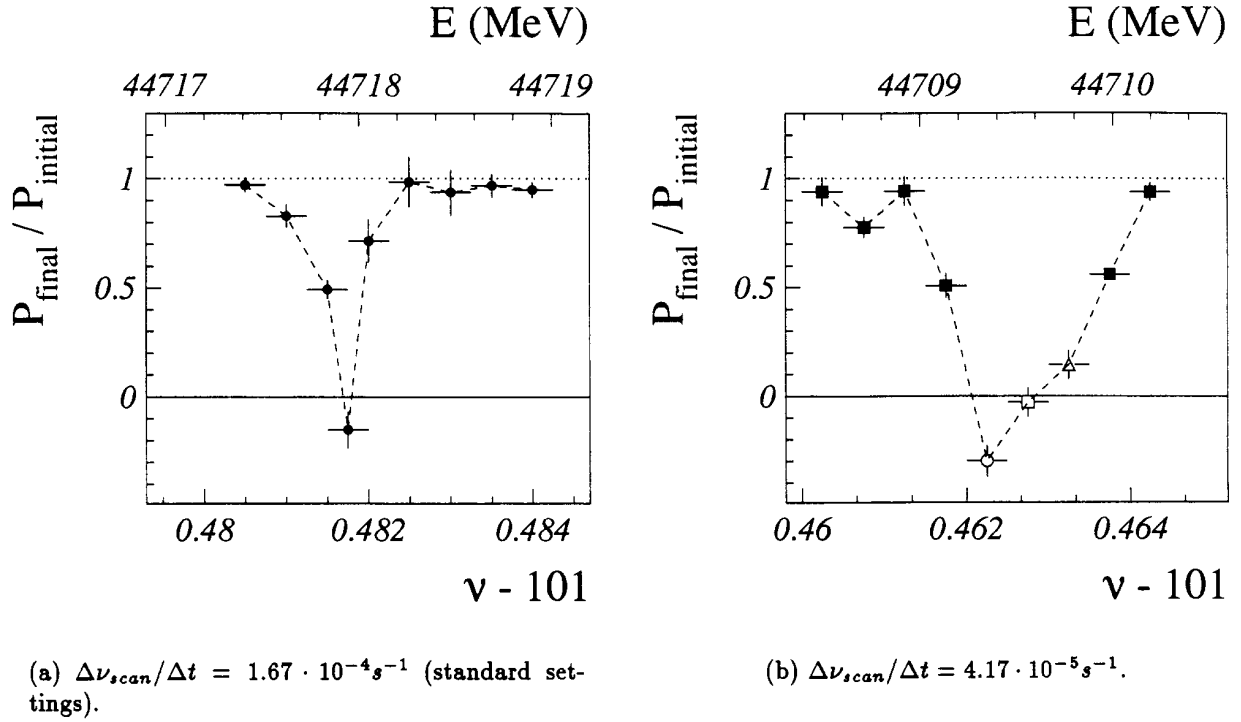


Figure 4: Two measurements of the artificially excited spin resonance are shown. Case (a) corresponds to a standard energy calibration. The slightly asymmetric resonance shape is due to tidal changes of the beam energy during the 12 minutes of measurement. In case (b) the slope of spin tune change with time is four times smaller and the resonance excitation is stronger. In this case different bunches were used to measure the resonance. They are indicated by different symbols.

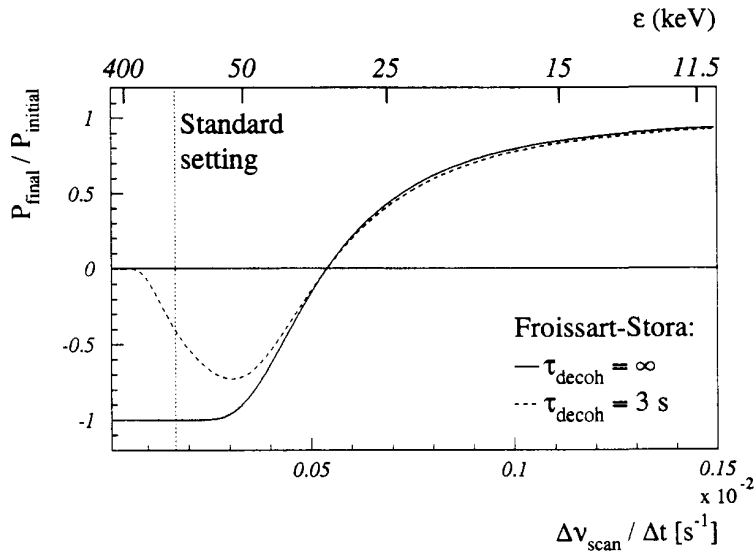


Figure 5: Calculated change in polarization $P_{final}/P_{initial}$ as a function of $\Delta\nu_{scan}/\Delta t$. On the upper scale the corresponding width of the excited spin resonance is indicated. The calculation was performed with a simple extension of the Froissart-Stora formula using the measurements from figure 4. It has been assumed that the field of the RF-magnet is $2 \cdot 10^{-3} \text{ Tm}$. The dotted line has been calculated for a decoherence time of 3 seconds.

the synchrotron radiation lead to a decay the horizontal component of the polarization with a decoherence time τ_{decoh} :

$$(5) \quad \frac{P_{\text{final}}}{P_{\text{initial}}} = e^{-T/\tau_{decoh}} [2 e^{-\chi} - 1]$$

$$(6) \quad \chi = \frac{\pi \epsilon^2}{2 \Delta \nu_{\text{scan}} / \Delta t}$$

T is taken as the time needed to cross the half-width of the excited spin resonance. In figure 5 the change in polarization $P_{\text{final}}/P_{\text{initial}}$ is shown for LEP as a function of $\Delta \nu_{\text{scan}}/\Delta t$ for this simple model. In this model a decoherence time of a few seconds explains why complete spin flips ($P_{\text{final}}/P_{\text{initial}} = -1$) have not been observed at LEP. For standard energy calibrations at LEP the width of the depolarizing resonance is sufficiently small to reach a precision better than 1 MeV and the depolarization is strong enough to be easily observed.

3.5 Interference between depolarizing resonances

It was suggested in [24] that interferences between the artificially excited spin resonance and natural spin resonances could result in a shift of the measured spin tune and a bias of the beam energy. The effect was studied experimentally by approaching strong natural spin resonances. The beam energy was changed by setting the RF-frequency f_{RF} to different values. For each setting the beam energy was measured by resonant depolarization. Any significant shift due to interference effects would disturb the expected relation between f_{RF} and the beam energy E in the vicinity of strong spin resonances :

$$(7) \quad \frac{\Delta E}{E} = -\frac{1}{\alpha} \frac{\Delta f_{\text{RF}}}{f_{\text{RF}}}$$

The momentum compaction factor α for LEP is calculated to be $1.859 \cdot 10^{-4}$ [12]. Its measurement with resonant depolarization is shown in figure 6. Though several strong spin resonances were crossed and $[\nu]$ was lowered down to 0.35 no significant deviation from the expected linear behavior was observed. The measured value of $\alpha = (1.860 \pm 0.020) \cdot 10^{-4}$ is in excellent agreement with the theoretical calculation. No significant shifts from interference effects were found in any experiment performed in 1993. From the experimental results any bias of standard energy calibrations due to interference of spin resonances can be excluded down to $\Delta E/E = 2 \cdot 10^{-6}$.

3.6 Spin tune shifts due to longitudinal magnetic fields

The relation between spin tune ν and beam energy E given by equation 3 is only valid in ideal storage rings without any longitudinal and radial magnetic fields. In LEP strong longitudinal fields arise from the experimental solenoids. Radial fields occur due to vertical closed orbit deviations mainly at the quadrupoles. Since three-dimensional rotations do not commute the relation from equation 3 is not strictly valid any more and small spin tune shifts $\delta\nu$ can occur. In the general case the spin tune is given by :

$$(8) \quad \nu = \frac{E[\text{MeV}]}{440.6486(1)[\text{MeV}]} + \delta\nu$$

$\delta\nu$ introduces a bias of the energy calibration. The effect was found to be small for the LEP experimental solenoids [25]. Around $[\nu] = 0.5$ the shift due to the solenoids is smaller than

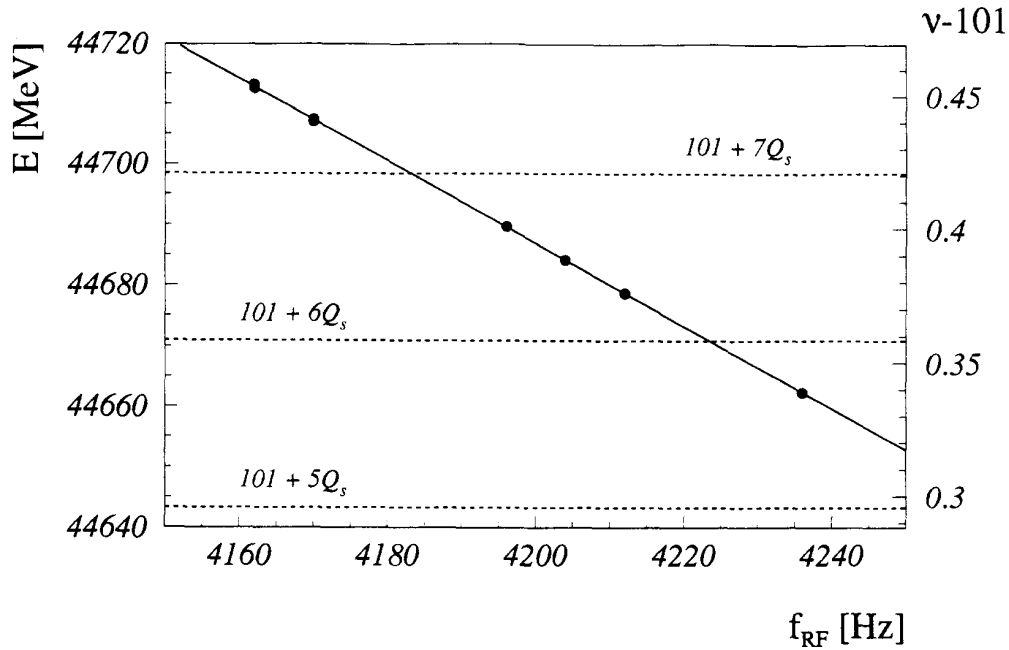


Figure 6: Measured beam energy E as a function of the RF frequency f_{RF} . Only the last four digits of f_{RF} are indicated. The nominal RF frequency used at LEP is 352 254 170 Hz. Two strong Q_s spin resonances indicated by the dotted lines were crossed during the measurement. No unexpected shifts of the beam energy were observed. The errors on the energy measurements are smaller than the symbols used in this figure.

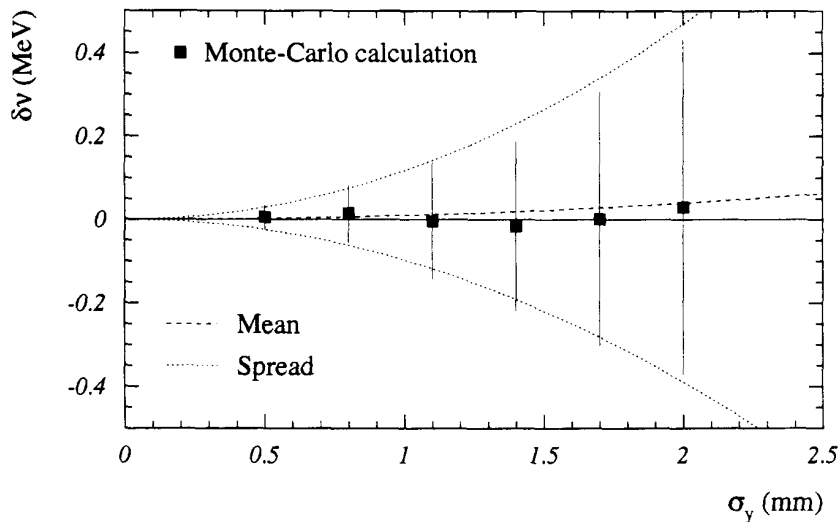


Figure 7: The mean spin tune shift and its spread due to radial magnetic fields are shown as a function of the RMS deviation of the vertical closed orbit σ_y for $\nu = 101.45$. The analytical calculations (smooth curves) are compared to Monte-Carlo results (black squares). The bars on the points give the spread from the Monte-Carlo calculation.

$\delta\nu = 10^{-4}$ without spin matching of the solenoids and smaller than $\delta\nu = 10^{-5}$ with spin matching.

The theoretical prediction was tested experimentally when the spin matching bumps for the solenoids were switched off after a successful spin tune measurement. The spin tune was immediately remeasured and found to be located in the same $\Delta\nu_{\text{scan}} = 0.002$ wide scan range than before.

3.7 Spin tune shifts due to radial magnetic fields

In a real storage ring the beam-line elements are not perfectly aligned. As a consequence the beam is subject to random radial error fields mainly at the quadrupoles which can cause spin tune shifts $\delta\nu$. This problem was treated in [26].

The radial fields produce spin rotations that do not commute with the nominal spin precession. A spin tune shift $\delta\nu$ can result with a RMS spread of :

$$(9) \quad \sigma(\delta\nu) \approx 0.04 \nu^2 n_Q (KL)^2 \sigma_y^2$$

where n_Q is the number of quadrupoles, σ_y the RMS distortion of the vertical closed orbit and KL the quadrupole strength. The effect from orbit correctors is neglected and $[\nu]$ is assumed to be close to 0.5. For accelerators with high beam energy $\delta\nu$ can become large.

This effect puts a practical limit on the accuracy of energy calibration by resonant depolarization for LEP. Numerical estimates predict an average spin tune shift of less than 10 keV for $\nu = 100.45$. The spread $\sigma(\delta\nu)$ is estimated to be about 30 keV for $\sigma_y = 0.5$ mm. The dependence of $\sigma(\delta\nu)$ on the vertical closed orbit RMS is illustrated in figure 7. At LEP the spin tune shift due to the finite vertical closed orbit is smaller than 100 keV for all practical cases. This introduces a relative uncertainty of $\Delta E/E < 2 \cdot 10^{-6}$ on the energy calibration.

The effect was studied experimentally by looking for unexpected changes of the spin tune after vertical closed orbit corrections. In one case a significant change in the beam energy between 0.4 MeV and 1.2 MeV was found. In another experiment a change by 0.1 MeV to 0.5 MeV was seen. For all other measurements no significant effect was observed. The experimental results are compatible with the calculated spread.

Harmonic Spin Matching was used routinely during energy calibration. This technique for polarization optimization uses vertical π -bumps [8] which could potentially produce spin tune shifts, but simulations show that their effect on the spin tune is totally negligible [12]. On one occasion the spin tune was measured with and without the Harmonic Spin Matching bumps and no shift was observed within the scan width of $\Delta E_{\text{scan}} = 0.88$ MeV.

3.8 Effects of electrostatic fields

Transverse electrostatic fields are used at LEP to separate the electron and positron beams at certain positions in the ring to avoid parasitic collisions. According to equation 2, transverse electrostatic fields affect the spin in a similar way than transverse magnetic fields. The differences are of the order of $\sim 1/\gamma$. Given the large γ factor ($8.8 \cdot 10^4$) of the LEP beams and the small strength of the electrostatic fields, spin tune shifts due to electrostatic field do not lead to any significant bias of the energy calibration.

3.9 Effects of quadratic non-linearities

Small systematic spin tune shifts can occur due to the spin tune spread related to synchrotron oscillations of the individual particles. This effect is expected to be very small. For LEP this

Source	$\Delta E/E$	ΔE ($E=45.6$ GeV)
Electron mass	$3 \cdot 10^{-7}$	15 keV
Revolution frequency	10^{-10}	0 keV
Frequency of the RF magnet	$2 \cdot 10^{-8}$	1 keV
Width of excited resonance	$2 \cdot 10^{-6}$	90 keV
Interference of resonances	$2 \cdot 10^{-6}$	90 keV
Spin tune shifts from long. fields	$1.1 \cdot 10^{-7}$	5 keV
Spin tune shifts from hor. fields	$2 \cdot 10^{-6}$	100 keV
Quadratic non-linearities	10^{-7}	5 keV
Total error	$4.4 \cdot 10^{-6}$	200 keV

Table 1: The accuracy of the beam energy calibration method by resonant depolarization is summarized for LEP. A standard energy calibration with a well corrected vertical closed orbit is assumed. All errors are understood to be RMS errors.

Source	$\Delta E/E$	ΔE ($E=45.6$ GeV)
Frequency of the RF magnet	$2 \cdot 10^{-6}$	0.1 MeV
Interference of resonances	$2 \cdot 10^{-6}$	0.1 MeV
Spin tune shifts from long. fields	10^{-5}	0.5 MeV
Spin tune shifts from hor. fields	$1.8 \cdot 10^{-5}$	0.8 MeV
Quadratic non-linearities	10^{-5}	0.5 MeV
Total upper bound	$2.4 \cdot 10^{-5}$	1.1 MeV

Table 2: Experimental tests of several systematic effects. The systematic errors in table 1 could only be verified with limited accuracy. Only an upper bound was established experimentally for the systematic error.

shift produces a relative error of $\Delta E/E < 1 \cdot 10^{-7}$ [7, 27]. The effect is controlled by variation of quadratic non-linearities, e.g. the chromaticity of radial betatron oscillations. To verify that this effect is not important for LEP, the chromaticity was increased by about +10 between two spin tune measurements. No change in energy was observed within ± 0.88 MeV.

3.10 Summary on the calibration accuracy

Systematic errors on an individual the energy calibration at LEP are summarized in table 1 for the different sources of uncertainties. The total systematic error on energy calibration by resonant depolarization is estimated to be about 0.2 MeV on the Z pole. The systematic error on calibration with resonant depolarization was obtained using theoretical studies. Experimental verification of these results could be performed with limited accuracy, as summarized in table 2. An experimental upper bound for the systematic error of 1.1 MeV was established. We estimate the systematic error to be better than 200 keV for a standard energy calibration in regular storage ring settings.

4 LEP settings for beam energy calibration

Operational energy calibrations were performed on the electron beam for three energies. The LEP settings are described in table 3 and are designated by Peak-2, Peak and Peak+2. Calibrations were performed with a minimum amount of modifications to the normal luminosity settings to reduce possible systematic effects. For an energy calibration at the end of a LEP physics fill, the following modifications were introduced :

- The positron beam is dumped. Only the last 4 calibrations were performed with both beams present in the ring. In these cases the two beams were vertically separated at the interaction points to avoid collisions.
- The betatron tunes are changed from the normal physics tunes $(Q_x, Q_y) = (90.26, 76.18)$ to special polarization tunes $(Q_x, Q_y) = (90.1, 76.2)$.
- The vertical and horizontal closed orbits are corrected to a small RMS ($\sigma_y \leq 0.3$ mm, $\sigma_x \leq 0.5$ mm).
- The polarization level is improved with Harmonic Spin Matching bumps.
- Vertical solenoid compensation bumps are introduced to compensate the spin rotation due to the experimental solenoids.

LEP Setting	Beam Energy (GeV)	CM Energy (GeV)	Spin Tune ν
Peak-2	44.72	$89.44 \approx m_Z - 2$	101.48
Peak	45.59	$91.18 \approx m_Z$	103.47
Peak+2	46.51	$93.02 \approx m_Z + 2$	105.54

Table 3: Definition of the three LEP settings and the corresponding typical beam and center-of-mass (CM) energies. m_Z is the Z boson mass. The precise beam energy for a defined calibration can vary due to different parameters that affect the LEP beam energy.

4.1 Effects of LEP settings on beam energy

Accelerator settings can modify the spin tune without affecting the energy, as has already been discussed, but they may also shift the beam energy. A number of experiments were performed to verify the effects of accelerator parameters on the energy.

4.1.1 PRETZEL ORBITS

Since 1992 LEP is colliding 8 electron and 8 positron bunches. To avoid beam encounters in the middle of the arcs, both beams evolve on horizontal pretzel orbits [28]. Particles on pretzel orbits make large horizontal betatron oscillations and if they were to stay on the same central orbit, the oscillations would lengthen their orbit by [29] :

$$(10) \quad \Delta C_c \simeq \frac{8q_x^2 x_p^2}{C_c} \simeq 0.1 \text{ mm}$$

where x_p is the pretzel amplitude and $q_x = 84$ is the horizontal tune inside the pretzel. In reality, the RF frequency forces the length of the orbit to remain constant and the average orbit position moves inward by $\Delta C/2\pi$ to satisfy this constraint. This would lead to a lower equilibrium energy of the beams, but the large orbit excursions in the sextupoles give additional contributions with the opposite sign. The net energy change was calculated to be +0.2 MeV [29].

In 1992 a measurement of the energy variation due to the pretzel orbits gave a rather large shift of $\Delta E = -1.7 \pm 0.7$ MeV [3, 29]. Two experiments were performed in 1993 at the end of normal calibrations and the results, shown in table 4, agree with the theoretical expectation.

Since calibrations at the end of physics fills were always performed with pretzel orbits, this is not a critical error. It only plays a role when Machine Development (MD) calibrations, often performed with normal orbits, are compared with the physics fills calibrations. It cannot be excluded that due to field imperfections and misalignments, the real energy shift from Pretzel can be different from the theoretical estimate.

4.1.2 BETATRON TUNES

Energy calibrations are performed with betatron tunes of $(Q_x, Q_y) = (0.1, 0.2)$ which differ from the standard physics tunes of $\sim (0.26, 0.18)$. This tune shift improves the pattern of depolarizing resonances close to $[\nu] = 0.5$ where the highest polarization is obtained [8]. To calibrate with physics tunes, a careful and delicate adjustment of the energy is required to reach

Experiment	ΔE (MeV)
1992 Measurement	-1.7 ± 0.7
LEP Fill 1674	$+0.1 \pm 0.6$
LEP Fill 1698	-0.4 ± 0.6
1993 Average	-0.2 ± 0.4
Theor. Estimate	+0.2

Table 4: Measurements of the energy change $\Delta E = E(\text{pretzel}) - E(\text{no pretzel})$ due to pretzel orbits.

a good level of polarizations and to avoid depolarizing resonances. In a dedicated MD, good polarization was obtained with tunes (0.25, 0.2) close to physics tunes. The energy difference between the horizontal tune settings was measured to be :

$$(11) \quad E(Q_x = 90.25) - E(Q_x = 90.1) = -0.2 \pm 0.6 \text{ MeV}$$

which shows that there is no significant bias due to the tune change.

4.1.3 LOW BETA OPTICS

The reduction of the betatron function β^* at the interaction point from 20 cm to 5 cm for luminosity running should not affect the energy. Normal energy calibrations are performed in the same low beta conditions than physics fills, but LEP is usually operated with $\beta^* = 20$ cm in MD experiments. The effect of lowering β^* could only be compared with different fills which introduces a systematic error of about 2.5 MeV. The observed energy change was :

$$(12) \quad E(\beta^* = 5\text{cm}) - E(\beta^* = 20\text{cm}) = 1.5 \pm 0.7 \pm 2.5 \text{ (fill-to-fill) MeV}$$

No effect of the β^* reduction was therefore observed within the large uncertainties.

4.1.4 LOCAL MAGNETIC BUMPS

A closed local magnetic bump does not change the beam energy : there is no net deflection of the beam and the change in path length does not lead to a significant change in energy. The effect of the horizontal bumps used to steer the beam in the interaction region between the Compton polarimeter laser and the electron bunches have been controlled. When a similar horizontal bump with an amplitude of 5 mm was introduced in another location of LEP, depolarization was observed in the same 0.88 MeV wide scan region than without the bump. Local beam steering is also used routinely between energy calibrations in a single fill without visible effect on the energy.

5 Models of energy variations and corrections

The beam energy of LEP is subject to fluctuations due to the LEP settings and to “environmental conditions”. Their impact on the energy can be minimized or corrected by a tight control of the running conditions (temperature and excitation of the magnets, RF frequency), a good understanding and prediction of the effects (tidal deformations) and a continuous monitoring of critical parameters (temperature, magnets currents). We will describe in this chapter some parameters that are necessary to compare energy calibrations and to correct the measurements to a define reference situation.

5.1 Magnetic field measurements

A measurement of the LEP bending field is provided by a NMR probe which is installed inside a reference magnet and read out every few minutes. This reference magnet is connected in series with the LEP main bending magnets. For the analysis of our data, the two closest NMR readings to a calibration with resonant depolarization have been averaged. The energy predicted from this average will be denoted by E_{NMR} . It can be used to track energy variations due to

Experiment	$\alpha[\times 10^4]$
LEP Fill 1717	1.862 ± 0.045
LEP Fill 1734	1.860 ± 0.020
Average	1.860 ± 0.018
Theory	1.859

Table 5: Measurements of the momentum compaction factor α for the $90^\circ/60^\circ$ lattice.

the main bending field inside a fill or between consecutive fills. Unfortunately, this instrument is not completely understood and it is not entirely clear if all the variations measured with the NMR correspond to true field changes. More details on the problems related to the NMR probe can be found in appendix A.

5.2 Momentum compaction factor

The momentum compaction factor α relates changes in the RF frequency f_{RF} or in the orbit length L_o to the energy of the beam :

$$(13) \quad \frac{\Delta E}{E} = -\frac{1}{\alpha} \frac{\Delta f_{RF}}{f_{RF}} = \frac{1}{\alpha} \frac{\Delta L_o}{L_o}$$

α depends on the horizontal focusing and one has the useful approximate relations [30] :

$$(14) \quad \alpha \cong \frac{\langle D_x \rangle}{R} \approx \frac{1}{Q_x^2}$$

where $\langle D_x \rangle \approx 70$ cm is the average horizontal dispersion in the arcs and R the average bending radius. The strong focusing produces a small momentum compaction factor. Tiny circumference variations produce observable energy variations because they are enhanced by about 4 orders of magnitude.

The momentum compaction factor was measured on two occasions. In a first experiment the RF frequency was changed by +38 Hz and the corresponding energy change was used to extract α . A second measurement was performed with a 75 Hz RF frequency scan (see figure 6 in a previous section). The results shown in table 5 are in agreement with the theoretical expectations of $\alpha = 1.859 \cdot 10^{-4}$ for the $90^\circ/60^\circ$ lattice obtained from simulation of LEP with the MAD program [31].

5.3 Terrestrial tides

Terrestrial tides of the sun and the moon move the earth surface up and down by up to ~ 25 cm in the Geneva area. This corresponds to a local change of the earth radius of $4 \cdot 10^{-8}$. The strain modifies the circumference C_c of LEP by 1 mm [32]. Since the length of the orbit is fixed by the constant RF frequency, the change in circumference will force the particles to move off-center in the quadrupoles where they receive an extra deflection. This leads to a change in beam energy ΔE [33] :

$$(15) \quad \frac{\Delta E}{E} = -\frac{1}{\alpha} \frac{\Delta C_c}{C_c}$$

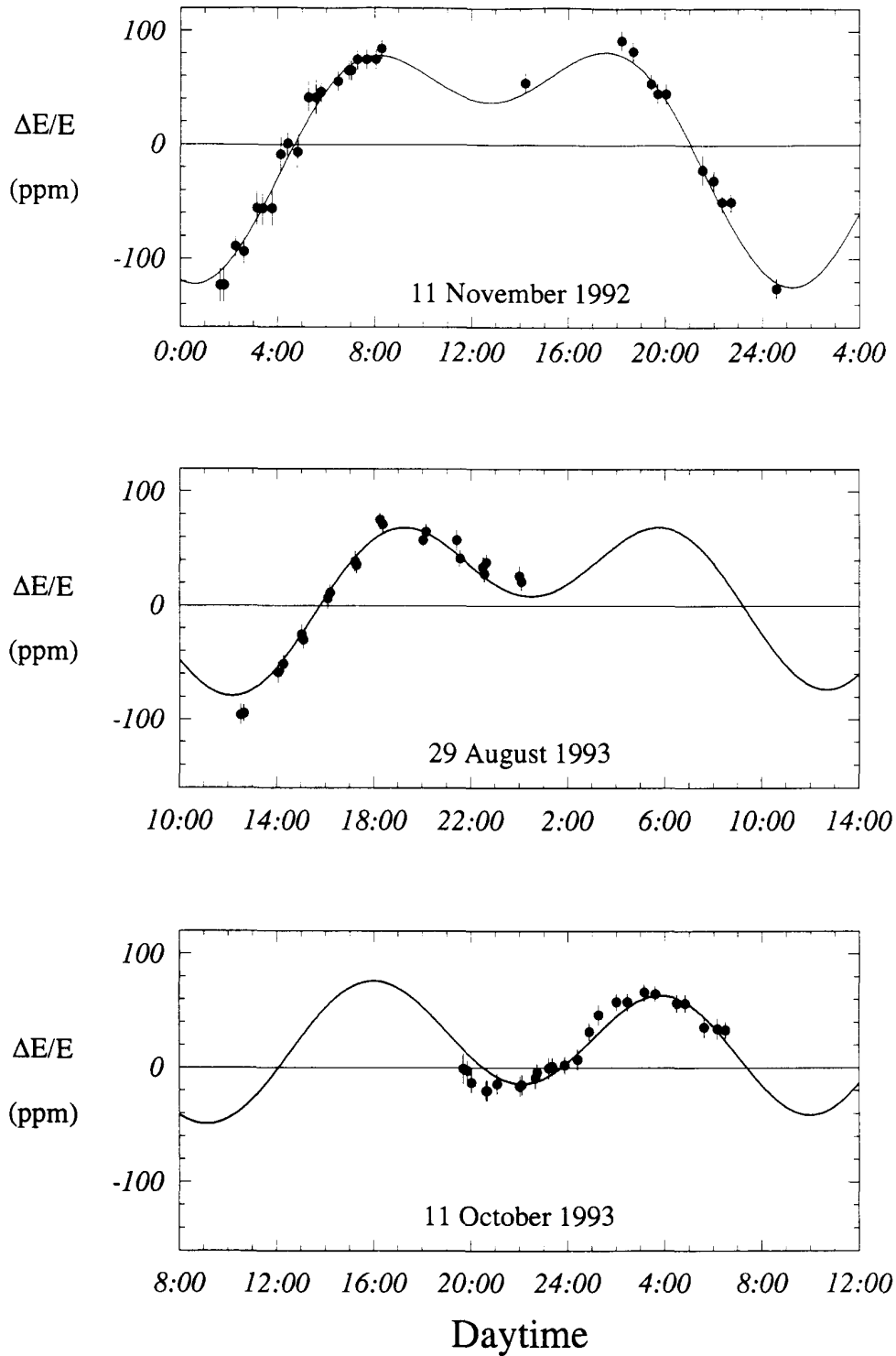


Figure 8: Evolution of the relative beam energy variation due to tides as a function of time in November 1992, August and October 1993. The solid line is the predicted evolution from the CTE tide model. The average value of κ_{tide} has been used in all pictures. The October 1993 experiment corresponds to a situation close to half moon, while the November 1992 experiment was performed during full moon.

In a good approximation, the horizontal strain is proportional to the change in gravity Δg , a quantity that can be predicted by computer codes with good accuracy [34]. The tide coefficient κ_{tide} relates Δg to ΔE :

$$(16) \quad \frac{\Delta E}{E} = \kappa_{tide} \Delta g$$

A high tide Δg exceeds 140 μgal in Geneva (1 gal = 1 cm s⁻²). A first experiment performed in November 1992 [33] showed excellent agreement between the measured energy variations and the prediction from a very simple tide model. In 1993 a more accurate CTE (Cartwright-Tayler-Edden potential [34]) tide model was adopted. This model, a harmonic development of the tide potential into 505 terms, includes empirical amplitude corrections and phases obtained from Earth tide measurements [35]. The results of 3 long and stable experiments are shown in figure 8. The energies follow the CTE tide predictions, with the exception of a few points that may indicate small uncontrolled energy fluctuations. Using all measurements the following value of κ_{tide} is extracted for the CTE model [36] :

$$(17) \quad \kappa_{tide} = (-8.6 \pm 0.8) \cdot 10^{-7} / \mu\text{gal}$$

where the error is estimated from the spread of the data and includes an estimate for uncertainties due to the use of the CTE potential to predict the tidal deformations. Measurements of Earth elasticity show that about 16% of the gravity variation couples into lateral strain. Using this information, we obtain an estimate for κ_{tide} :

$$(18) \quad \kappa_{tide} \approx \frac{-0.16}{\alpha g_0} = -9 \cdot 10^{-7} / \mu\text{gal}$$

where $g_0 = 980$ gal is the average local gravity. This estimate is in good agreement with our measurements. More details on the tide effects can be found in [34, 36].

5.4 Magnet temperature

The bending field of the LEP dipoles has a significant dependence on the magnet core temperature because of the iron-concrete structure of the magnets [5]. We define the temperature coefficient α_T as :

$$(19) \quad \alpha_T = \frac{1}{E} \frac{\Delta E}{\Delta T}$$

where T is the average temperature of 32 out of 3300 dipole cores. The 32 sensors are evenly distributed in all octants.

The temperature coefficient α_T of the LEP dipoles was measured on 3 occasions using resonant depolarization :

- **Experiment 1 (fill 1636)** : The average temperature of the LEP dipoles increased by $\sim 0.3^\circ\text{C}$ in 4 hours. The correlation between the beam energy and the temperature is shown in figure 9.
- **Experiment 2 (fill 1734)** : The average temperature of the LEP dipoles increased by $\sim 0.4^\circ\text{C}$ during this energy scan experiment. α_T was extracted together with the momentum compaction factor α . The residual energy variation after correction for RF frequency shifts is shown as a function of temperature in figure 10.

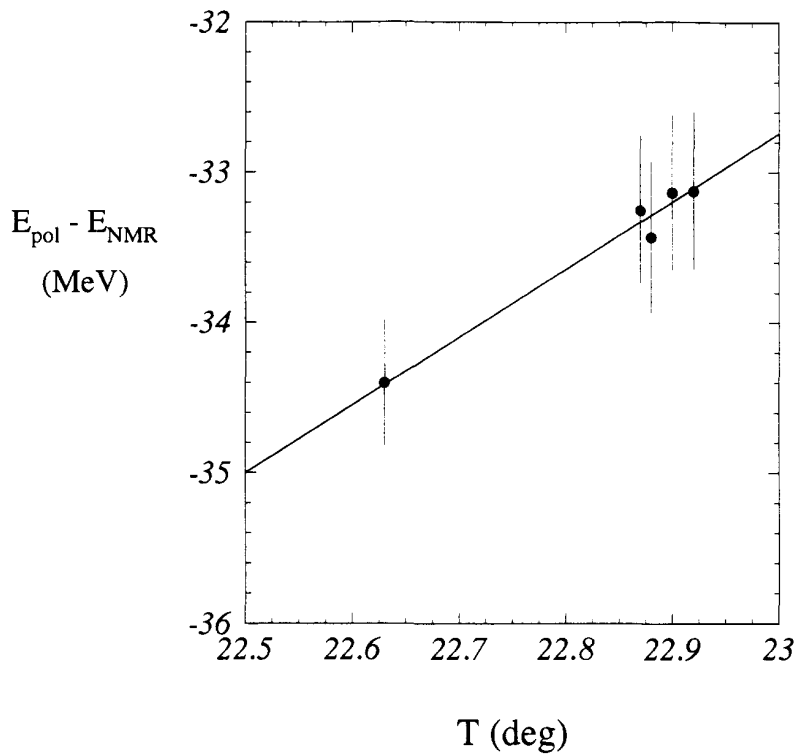


Figure 9: Correlation between the average magnet temperature and the tide corrected beam energy in fill 1636.

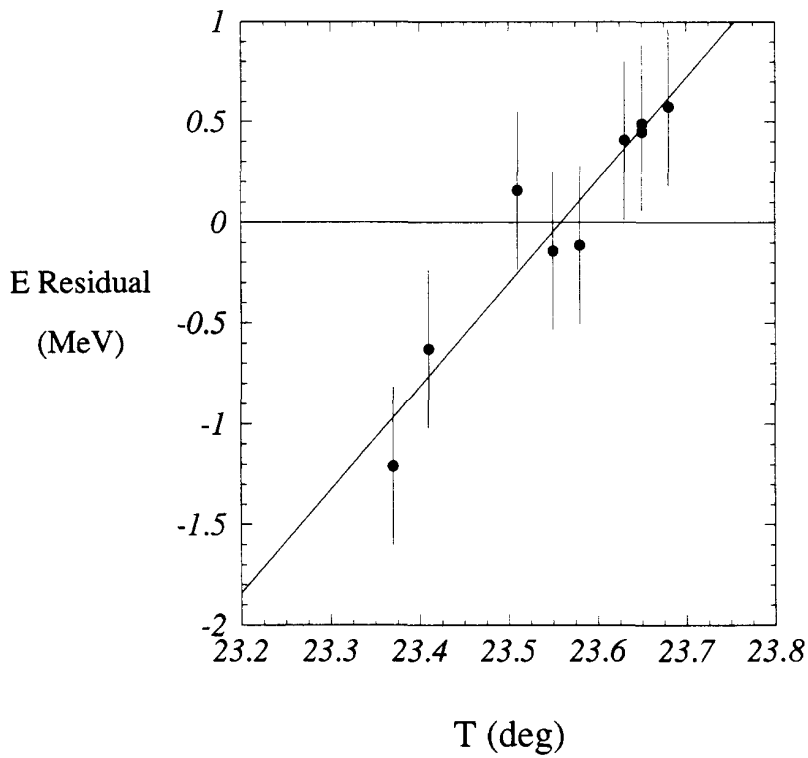


Figure 10: The residual energy variation (after correction for RF frequency changes and tides) is shown as a function of the average magnet temperature (fill 1734).

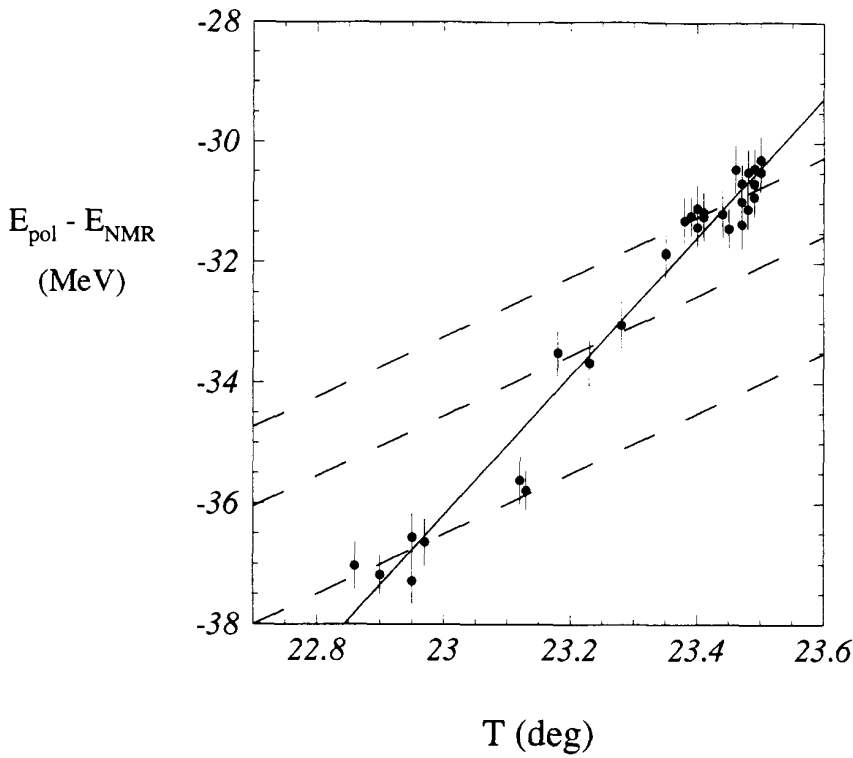


Figure 11: Correlation between the energy and the magnet temperature for fill 1772. The solid line corresponds to a fit to the whole data set with a slope of $2.5 \cdot 10^{-4}$. The dashed lines show the expected correlation inside each group of data between the possible energy jumps (figure 12) with a slope of $1.1 \cdot 10^{-4}$.

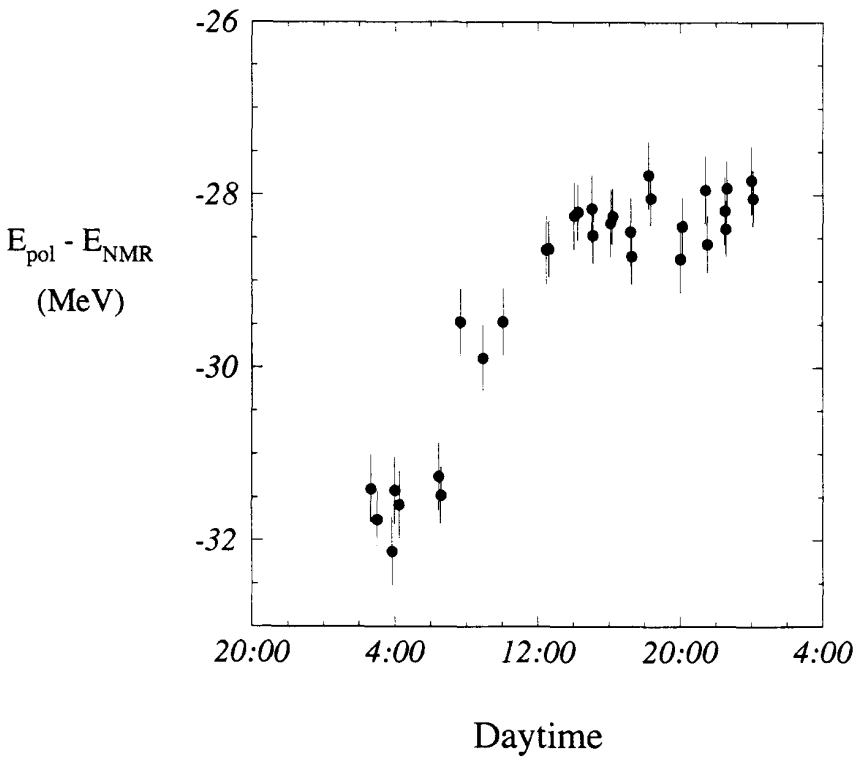


Figure 12: Evolution of $E_{pol} - E_{NMR}$ in fill 1772. The energies have been corrected for tide, RF frequency and temperature (coeff. from table 6). There are indications for 2 sudden energy jumps.

Experiment	$\alpha_T [10^{-4}/\text{deg}]$
LEP fill 1636	1.01 ± 0.43
LEP fill 1734	1.12 ± 0.41
Average	1.07 ± 0.30

Table 6: Measurements of α_T .

- **Experiment 3 (fill 1772)** : This experiment was performed while the LEP magnets were warming up after a technical stop and the temperature increase was $\sim 0.6^\circ\text{C}$. If the full data sample is used for the temperature analysis as shown in figure 11, α_T reaches a value of $2.5 \cdot 10^{-4}$ with quite a good correlation between energy and temperature. This coefficient is about twice as large as the value extracted from the two first experiments.

When the data is corrected with the temperature coefficient obtained from the previous two experiments (table 6), the time evolution of the corrected energy is relatively flat with the exception of two sudden jumps (figure 12). Although there are indications to correlate these jumps with orbits corrections and small tune adjustments ($\Delta Q_x \sim 0.02$), it is not understood if those corrections were the cause of those jumps or if the energy jumps demanded these adjustments. An analysis of the beam orbits revealed no orbit movement that could explain an energy jump [37].

If the hypothesis of the 2 jumps is accepted, all the temperature data becomes consistent. But it is also the only occasion in 1993 when large ($> 1 \text{ MeV}$) and abrupt energy changes were observed inside a single fill. The origin and frequency of such jumps is unknown.

The analysis of the temperature data in fill 1772 has turned out to be very subtle due to the possible jumps in energy and we use the values of table 6 for the beam energy data analysis. The coefficients in table 6 are in agreement with other measurements [5]. They do not improve the precision already obtained previously because of the small temperature lever arms in the fills.

5.5 QFQD compensation loop

When LEP is running with different phase advances in the horizontal and vertical planes ($90^\circ/60^\circ$ optics), the excitation current in the F quadrupoles (hor. focussing) is larger than in the D quadrupoles (hor. defocussing). The two bars that carry the quadrupole excitation current run next to the LEP ring at a distance of about 1 m from the vacuum chamber and they are almost in the plane of the ring. To cancel the magnetic field created by the current asymmetry, a compensating current I_{Qfd} is flowing in a third bar next to the two others. The sum of all three currents should be zero, but during the 1993 LEP run, I_{Qfd} has been inverted or turned off on different occasions.

When I_{Qfd} is zero, the net current in the bars is about 33 A. A wire carrying such a current creates a field of $6.6 \mu\text{T}$ at the position of the beam in the vacuum chamber. The effective length over which this field is acting was estimated to be about 3750 m and corresponds to a bending strength of $\sim 0.025 \text{ Tm}$ for 33 A [38, 39].

The effect of I_{Qfd} was measured on two occasions by inverting I_{Qfd} from 32 A to -39 A . Reversing the current in the loop induced a change $\Delta E = -3.0 \pm 1.4 \text{ MeV}$ on average, in

Experiment	C_{Qfd} (MeV/A)
LEP fill 1845	0.025 ± 0.009
LEP fill 1888	0.062 ± 0.010
Average	0.042 ± 0.020
Theor. Estimate	0.037 ± 0.008

Table 7: Correction factor C_{Qfd} for the effect of the quadrupole current asymmetry. The error on the average is estimated from the spread of the 2 fills.

agreement with the theoretical estimate of -2.6 ± 0.5 MeV [38], but the two individual measurements show a significant difference. The error has been estimated conservatively from the spread of the two experiments. The correction coefficient C_{Qfd}

$$(20) \quad \Delta E = C_{Qfd} \Delta I_{Qfd}$$

is given in table 7.

5.6 Energy calibration reproducibility and correction quality

On most occasions, the beam energy was measured repeatedly during the same fill. This allows to estimate the reproducibility of the energy calibration and the quality of the correction factors. For this analysis, each energy measurement is corrected to a reference situation for all parameters that are known to affect the energy. We define for each corrected energy E the deviation δ_E :

$$(21) \quad \delta_E = \frac{E - E_{av}}{\Delta_E}$$

where E_{av} is the average corrected energy in a given the fill and Δ_E the half-width of the particular depolarization scan. The distribution of δ_E is expected to be flat between -1 and $+1$ if the measurements are uncorrelated and the energy is varying sufficiently between different depolarizations. When two calibrations are too close together in time (less than 15 mins) and without any change in beam conditions, the second calibrations is not used for the analysis to avoid a too strong bias towards $\delta_E = 0$. The experimental distribution, shown in figure 13, exhibits a roughly Gaussian shape instead of the expected flat distribution. There are a few reasons for the difference :

- When the energy of the beam is close to the edge of the depolarization scan, some depolarization is also observed in the neighboring scan region because of the width of the excited spin resonance. Usually the scan limits are then displaced to center the bin around the beam energy and to get a clean depolarization in only one scan. This attitude tends to bias δ_E towards 0 and to decrease the RMS.
- Some of the measurements are taken close together. In that case, the energy does not change much between two calibrations which are then strongly correlated.
- If the energy of the beam fluctuates because of effects which are not under our control or not monitored, the distribution will acquire tails beyond -1 and $+1$.

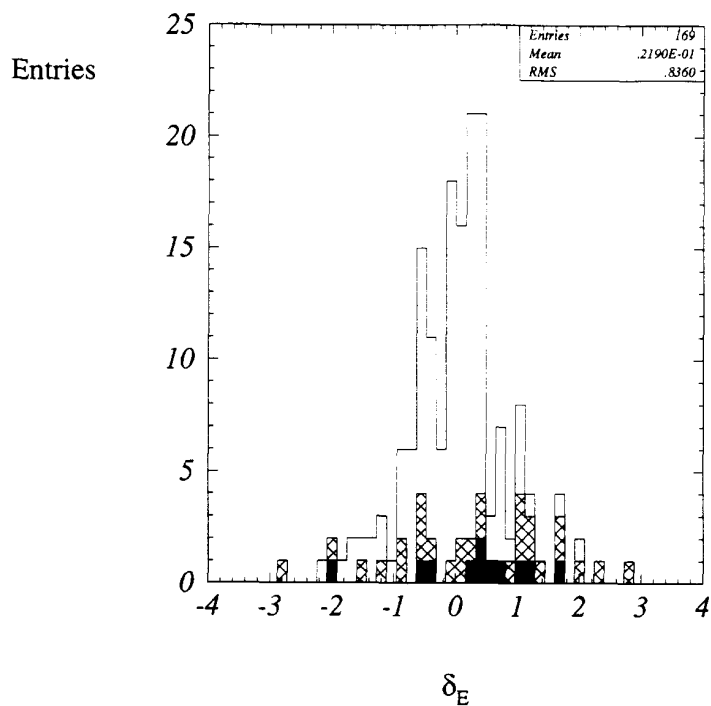


Figure 13: Distribution of δ_E for all the 1993 data. The RMS of the full distribution is 0.84. The histograms that are shown contain data with $\Delta_E = 0.11$ MeV (dense hatch), $\Delta_E \leq 0.22$ MeV (light hatch) and the full sample (white).

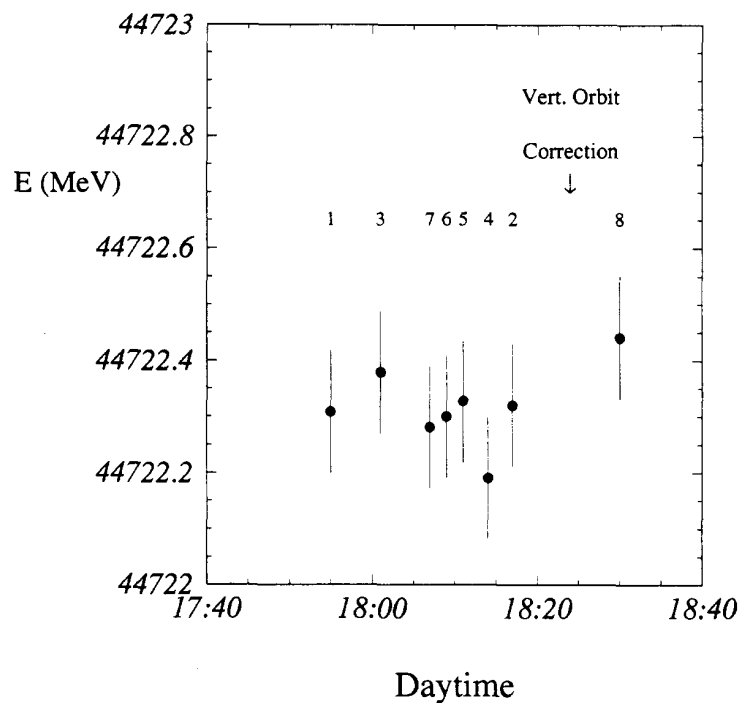


Figure 14: Comparison of the energies of different bunches (indicated by the numbers above the points). The energies shown as a function of time are corrected for all parameters known to affect the energy. The bunch currents were distributed between $85 \mu\text{A}$ (bunch 7) and $115 \mu\text{A}$ (bunch 6). The errors shown here correspond to the width of the frequency scan ($\pm\Delta_E$).

Experiment (LEP fill)	Date	Duration (hours)	Reproducibility
1636	20-06-93	4	Better than 0.3 MeV
1734	5-08-93	4.5	Better than 0.2 MeV
1772	29-08-93	21.5	2 and 1.3 MeV jumps, up to 0.8 MeV deviations
1811	12-09-93	5.5	0.6 MeV jump
1849	11-10-93	11	up to 0.8 MeV deviations

Table 8: Medium term beam energy measurement reproducibility.

The δ_E distribution of figure 13 has an RMS of 0.84 while the RMS of a flat distribution is expected to be $1/\sqrt{3} = 0.57$. The difference can be attributed to a systematic error σ_δ of 0.6. This corresponds to a typical systematic point to point error of $\simeq 0.3$ MeV on each measurement. We use this estimate to define for each individual calibration inside a fill the error on the energy :

$$(22) \quad \sigma_E = \sqrt{\frac{\Delta_E^2}{3} + (0.3 \text{ MeV})^2}$$

This relation includes reproducibility and correction errors and was used in this report to obtain the RMS error on an individual calibration with respect to the other calibrations of the same fill. For a standard calibration $\Delta_E = 0.44$ MeV, leading to $\sigma_E = 0.4$ MeV.

The energies of different bunches were compared during stable conditions and were identical within ± 100 keV over a 30 minutes time interval (figure 14). This experiment shows an excellent short term reproducibility of the beam energy calibration.

The medium term reproducibility of the beam energy measurement inside a single fill (6-24 hours) is typically ~ 0.5 MeV. Some steps or deviations of this importance are observed occasionally when the energy is tracked for some hours. A summary of such observations is given in table 8. Some of the jumps are visible in figures in this document. While there are indications to correlate several of these jumps to orbit corrections, those correlations are not sufficiently clear to apply a correction algorithm.

6 Positron beam energy

A positron polarimeter was installed during the LEP September 1993 technical stop and commissioned in the following months. The same laser beam that is used to measure the electron beam polarization is reflected back by a concave mirror to allow head-on collisions with the positron beam. The backscattered Compton photons are detected in a detector ~ 390 m downstream from the interaction point between the positron bunches and the laser beam. Unfortunately the operation of the system was more difficult than anticipated. Large fluctuations were observed in the rate of Compton photons scattered from the positron beam within a few seconds. It is believed that oscillations of the mirrors due to vibrations of the vacuum chamber

produced important changes in the position of the laser focus and could be at the origin of the effect. This problem should be solved in 1994.

It was still possible to perform a single test calibration when both electron and positron beams were present in LEP with a polarization of $\sim 15\%$. The energy of the electron beam was first carefully measured. Then the positron beam was depolarized. A shift with respect to the expected energy from the electron calibration was observed. Finally the calibration of the electron beam was confirmed. Due to a lack of time, it was not possible to change Q_s and f_{RF} to solve the ambiguities of the depolarization procedure for the positron beam. For this reason, it is only possible to give the following range for the difference of the energies :

$$(23) \quad 0.5 \text{ MeV} < | E_{e^-} - E_{e^+} | < 3.2 \text{ MeV}$$

The cause for this energy shift is not known and more experiments are planned in 1994 to understand the positron energy.

7 Beam energy calibration results in 1993

To combine the 1993 energy calibrations, all results are corrected to a reference situation for LEP defined in table 9. The reference RF frequency corresponds to the setting used in normal physics fills. The reference magnet temperature was chosen to be close to the average calibration temperature. For a given fill, all energies are corrected to the reference situation before the weighted average is calculated. The average correction for each parameter is used to obtain the contribution to the error on the energy due to the uncertainties on the correction coefficients. Numerical results for the calibration of all fills are given in appendix B.

In figure 15 the evolution of the energy E_{pol} obtained from resonant depolarization is shown as a function of time, corrected to the reference values of table 9. Two constant offsets have been subtracted from the energies at Peak+2 and Peak-2 to make the energies coincide on average at the begin of the LEP energy scan. The two energy points evolve in parallel, but they do not show the same amplitude of the variation as a function of time.

If the bending field of the main dipoles is the cause of the energy variations seen in figure 15 and if the NMR probe tracks this field correctly, the difference $E_{pol} - E_{NMR}$ should be constant over time. Figure 16 shows that this is not the case. The variations are roughly the same than for E_{pol} alone.

Parameter	Reference value	Correction factor
RF frequency	352 254 170 Hz	$\alpha = (1.860 \pm 0.020) \cdot 10^{-4}$
Tide	0 μgal	$\kappa_{tide} = (-8.5 \pm 0.8) \cdot 10^{-7} / \mu\text{gal}$
Av. Magnet Temperature	24°C	$\alpha_T = (1.1 \pm 0.3) \cdot 10^{-4} / \text{deg}$
QFQD comp. loop (Peak-2)	+32 A	$C_{Qfd} = (4.2 \pm 2.0) \cdot 10^{-2} \text{ MeV/A}$
QFQD comp. loop (Peak+2)	+33 A	

Table 9: Reference values of the parameters that affect the LEP beam energy. The correction factors used to correct E_{pol} are given in column 3.

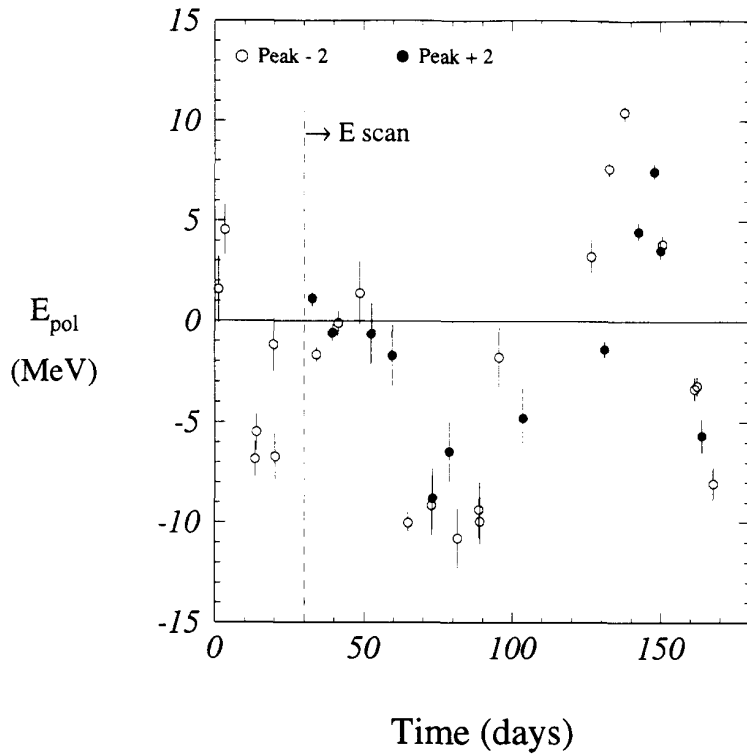


Figure 15: Evolution of the energy measured by resonant depolarization as a function of time in 1993. The time scale starts on June 1st 1993. The energies for Peak-2 and Peak+2 have been shifted to be roughly identical at the beginning of the energy scan.

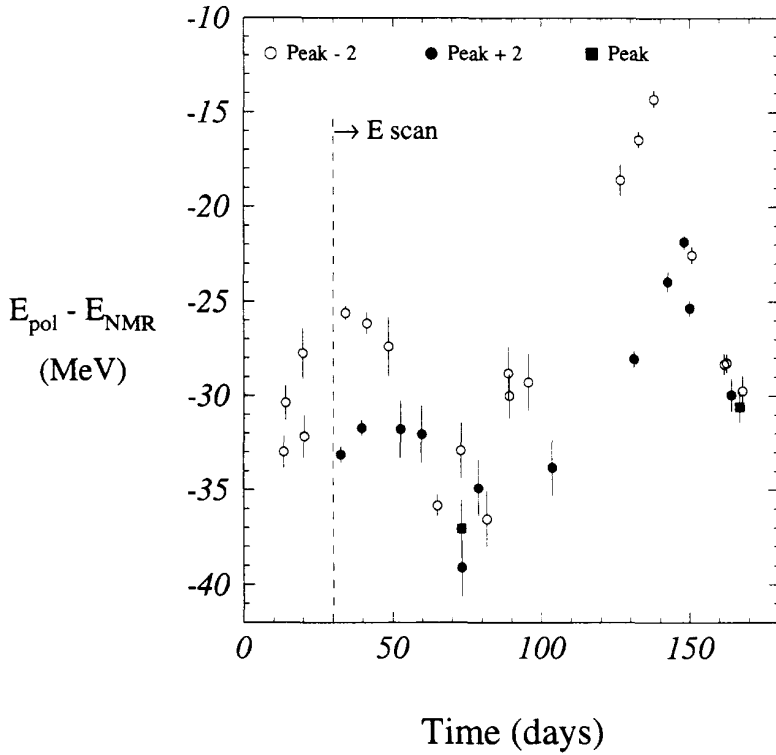


Figure 16: Evolution of the difference between the energy measured by resonant depolarization and by the NMR as a function of time.

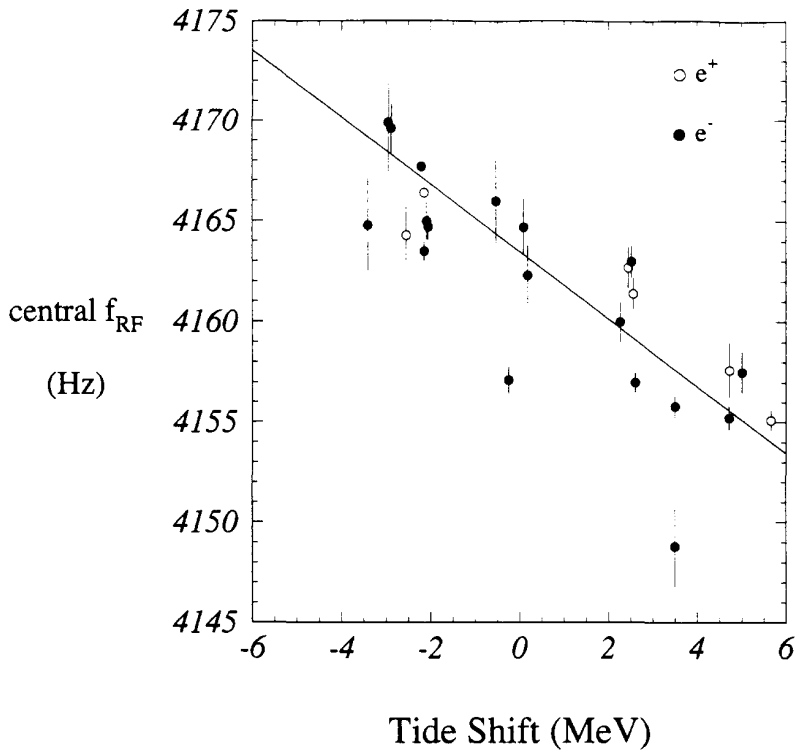


Figure 17: Correlation of the central RF frequency and the expected energy shift from tides. Only the last 4 digits of the frequency are shown on the axis.

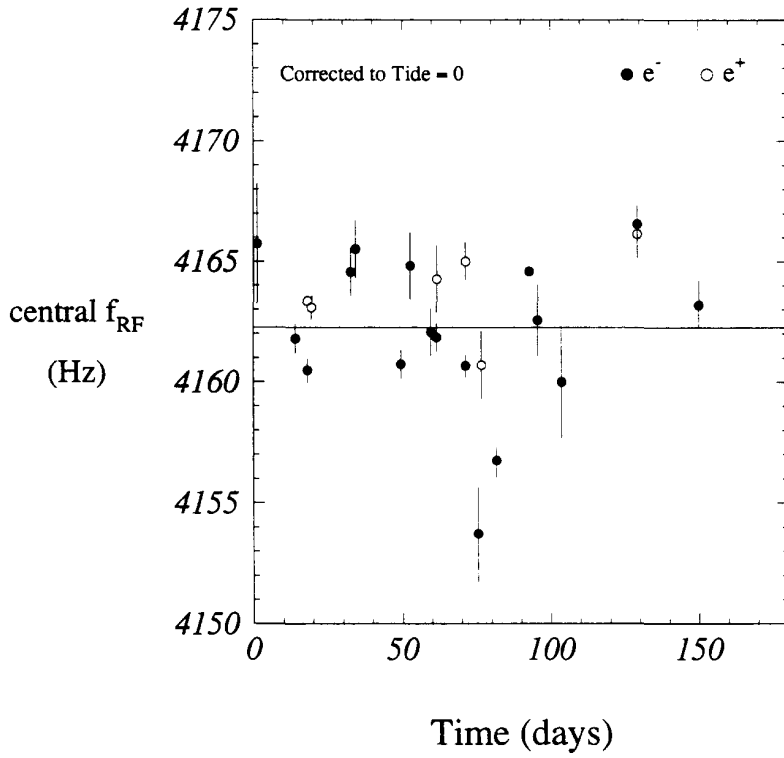


Figure 18: Evolution of the tide-corrected central RF frequency as a function of time. Conversion factor : 1 Hz \simeq 0.7 MeV.

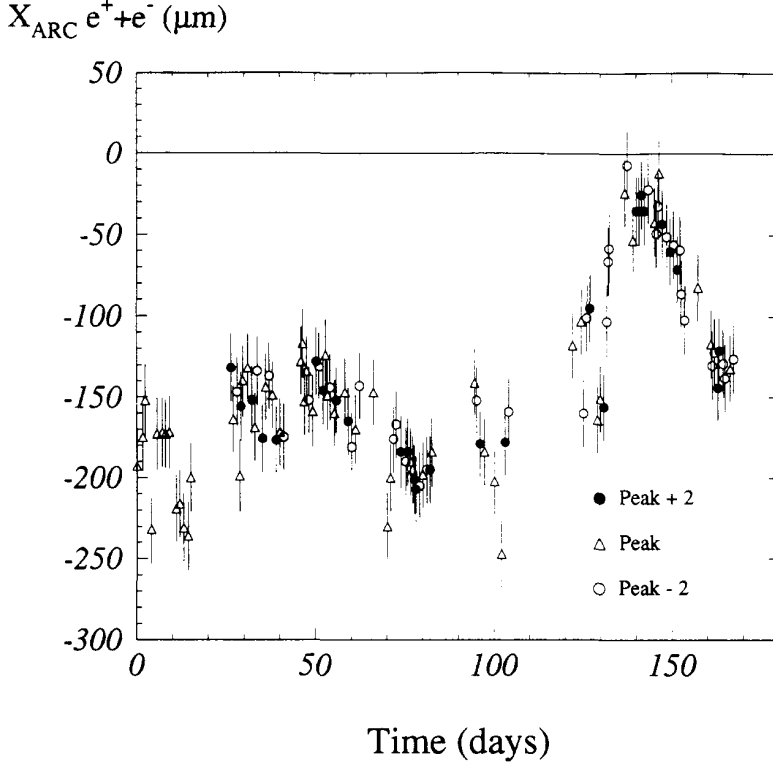


Figure 19: Evolution of the radial orbit position in the LEP arcs (average for both particles) as a function of time in physics fills. There is a large shift in the position which is correlated with the energy variations observed by the resonant depolarization calibrations. As expected the orbit evolution is identical for all energies.

A particle on the central orbit moves on average through the center of all the quadrupoles and sextupoles. On this orbit the net bending field from quadrupole and sextupole magnets vanishes. The central RF frequency f_{RF}^c corresponds to the RF frequency setting which brings the beams on the central orbit. A change of the circumference of LEP or a drift of the RF frequency, that could also explain the energy drift, can be directly measured with f_{RF}^c [40, 41]. The observed values of f_{RF}^c show the expected correlation with the tides (figure 17), but the spread of the data is larger than the measurement errors, which could be due to ring movements that are not due to tides. The evolution of f_{RF}^c as a function of time shows no evidence of a large change in the LEP circumference (figure 18). Unfortunately measurements are missing in the critical period of the largest energy drifts. In the absence of tides the average central RF frequency is :

$$(24) \quad f_{RF}^c (\Delta g = 0) = 352\,254\,162.6 \pm 2.5 \text{ Hz}$$

which corresponds to a LEP circumference of :

$$(25) \quad C_c (\Delta g = 0) = \frac{c h}{f_{RF}^c (\Delta g = 0)} = 26655.4686 \pm 0.0002 \text{ m}$$

where $h = 31320$ is the harmonic number of the LEP accelerating RF system and c is the velocity of light. The central beam revolution frequency is 11 246.94 Hz.

With the improved electronics of the Narrow Band LEP Beam Orbit Monitors (BOMs) [10, 11], an analysis of orbits measured during all LEP physics fills was performed [37]. The variations of the average radial beam position ΔX_{ARC} at the arc pickups and of the energy ΔE are

related through :

$$(26) \quad \Delta X_{ARC} = D_x^{p_u} \frac{\Delta E}{E} \cong 12.5 (\mu\text{m}) \cdot \Delta E[\text{MeV}]$$

$D_x^{p_u} \cong 57$ cm is the average horizontal dispersion at the pickups. Ring deformations force the beam to change its position in the quadrupoles and in the BOM pickups and induce a change in energy due to the bending field in quadrupoles and sextupoles. The terrestrial tides are an example of such deformations that are now well understood. The analysis of X_{ARC} reveals a drift of the beam position that is correlated with the evolution of E_{pol} (figure 19). When the beam energy is corrected for the movement of the orbit according to equation 26, the residual variations are significantly reduced (figure 20 and table 10). There are indications that the ring deformations are correlated with rainfall [42, 43].

The Flux-Loop consists of electrical loops threading all LEP dipoles which allow to measure the integrated bending field of the LEP dipole magnets [44, 45]. It has been used extensively for LEP energy calibration [5]. The Flux-Loop calibrations are insensitive to the effects of static magnetic fields and of the quadrupole and sextupole magnets on non-central orbits. For this reason, the measured Flux-Loop energies E_{fl} have been corrected by $+12 \pm 8$ MeV to account for aging of the concrete-iron dipole magnet cores, for the Earth magnetic field and for the effect of Nickel layer in the LEP vacuum chamber [46]. The Flux-Loop data has also been corrected by -5.2 MeV to account for the difference between the reference RF frequency of 352 254 170 Hz and the average tide-corrected central frequency. The total correction on E_{fl} is $+6.8 \pm 8$ MeV. Figure 21 shows that Flux-Loop and resonant depolarization calibrations agree within the errors. The two calibration methods are compared in table 10. The RMS of the difference is ~ 4.7 MeV, which corresponds to a precision of the Flux-Loop calibration of $\sim 10^{-4}$.

For resonant depolarization calibrations the betatron tunes were carefully set to $(Q_x, Q_y) = (0.1, 0.2)$. If a beam energy change is induced by magnetic fields, the strength of the quadrupole magnets will be mismatched and the betatron tunes will vary. The resulting correlation between tunes and energy was observed in [37], where the tune change was tracked by the excitation current of the arc quadrupoles required to set the tunes to their nominal values. Figure 22 shows the resulting correlation between the measured beam energy and quadrupole current for the 1993 data. The good correlation shows that the remaining energy variations are consistent with being due to magnetic fields within about ± 2.5 MeV. The combination of the beam orbit position in the arcs and the quadrupole current can therefore be used to track and understand the evolution of the beam energy in every fill [37].

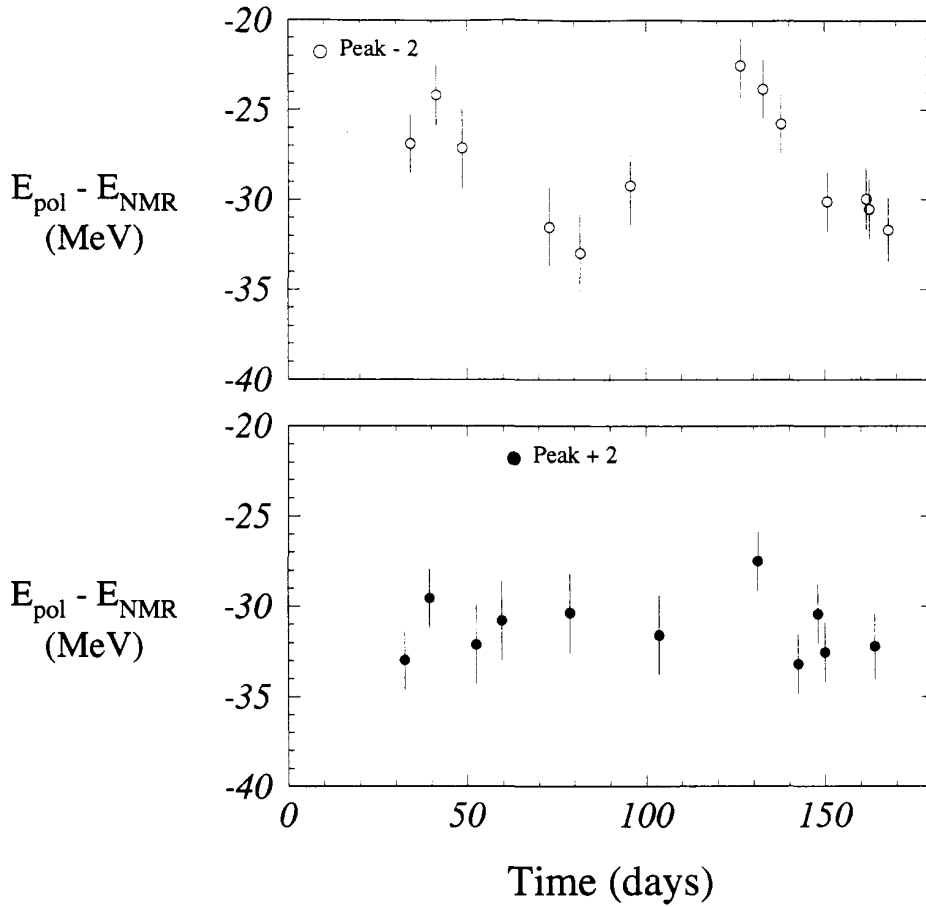


Figure 20: Evolution as a function of time of the beam energy after correction for the radial orbit movement shown in figure 19. Only calibrations performed in normal conditions at the end of physics fills are shown in these figures. The RMS spread of the data points is 3.4 MeV for Peak-2 and 1.7 MeV for Peak+2.

Quantity	Average (MeV)	RMS (MeV)
$E_{fl} - E_{NMR}$ (45 GeV)	-27.9 ± 1.7	5.3
$E_{pol} - E_{NMR}$ (Peak-2)	-28.9 ± 0.8	3.4
$E_{pol} - E_{NMR}$ (Peak+2)	-31.2 ± 0.5	1.7
$E_{fl} - E_{pol}$ (Peak-2)	-1.8 ± 1.5	4.8
$E_{fl} - E_{pol}$ (Peak+2)	$+0.4 \pm 1.5$	4.6

Table 10: Comparison of Flux-Loop and resonant depolarization calibrations. E_{pol} is corrected for the orbit movement observed with the BOM system. In each case, a systematic error of ± 8 MeV has to be added to E_{fl} . For the differences $E_{fl} - E_{pol}$, E_{pol} was averaged using the 2 closest measurements before and after a Flux-Loop calibration.

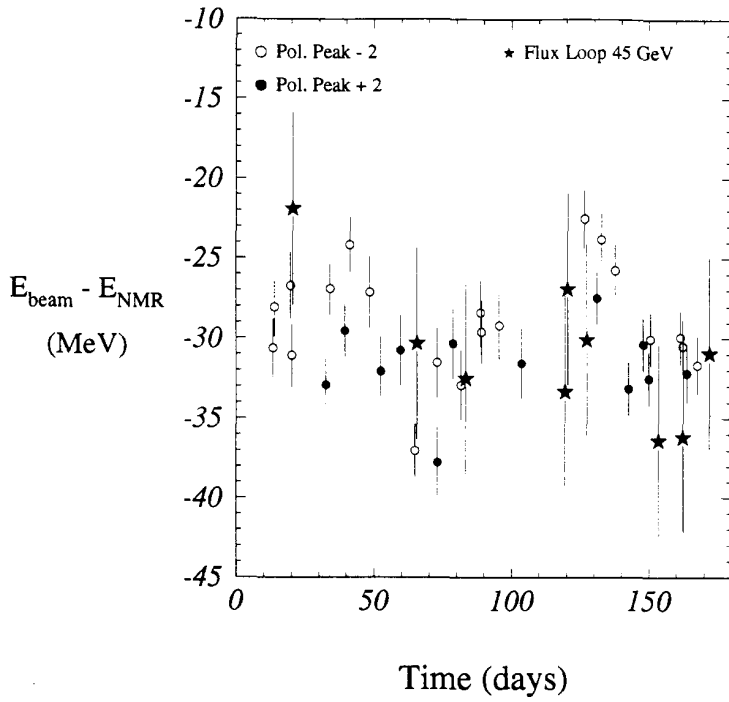


Figure 21: Comparison of all the LEP energy calibration by resonant depolarization and by the Flux-Loop. E_{pol} has been corrected for the radial orbit movement shown in figure 19. There is an additional error of ± 8 MeV on the absolute scale of the Flux-Loop data which is not shown.

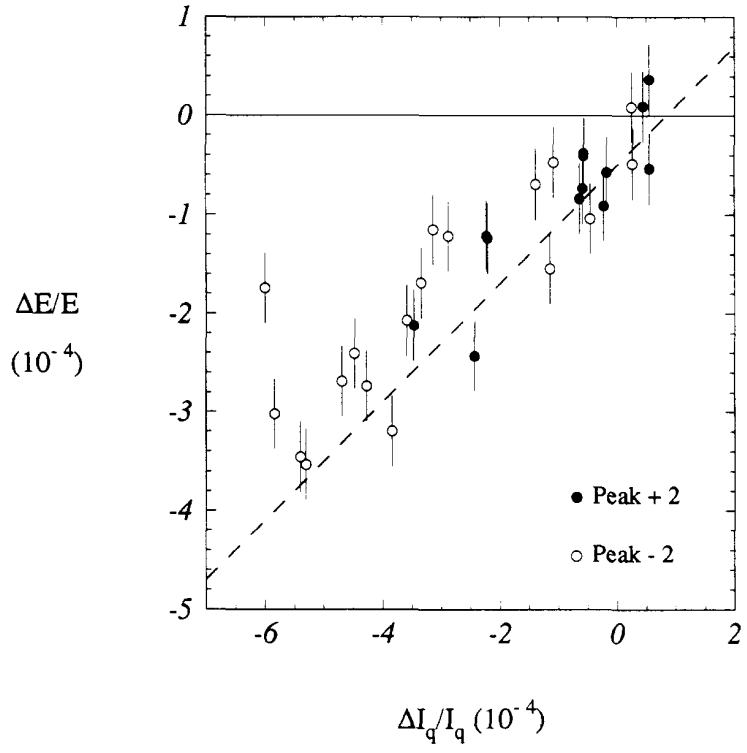


Figure 22: Correlation between the relative change in energy and in quadrupole excitation current. The beam energy is corrected for tidal deformations and for the orbit movement shown in figure 19. The dashed line corresponds to the expected slope of ≈ 0.6 . The good correlation shows that the remaining energy variations are due to magnetic bending fields within ± 2.5 MeV.

8 Conclusions

The energy calibration program of 1993 has provided a wealth of data on the behavior of the LEP beam energy. Some important points include :

- Operational energy calibration was successfully commissioned for 3 energies and 24 energy calibrations were performed at the end of physics fills within 3 to 4 hours.
- Several systematic effects have been studied in detail and the systematic error on a single energy calibration was shown to be smaller than 1.1 MeV.
- The energy dependence of the LEP beams on different physical parameters have been determined.
- A first test measurement of the positron beam energy was performed, indicating a possible difference between electron and positron energies.
- Unexpected energy variations of up to 20 MeV have been monitored in the course of the year.

A surprising aspect of the 1993 beam energy data is the rather large variation of up to 20 MeV (4×10^{-4}) observed between August and October. Part of this variations can be attributed to a change in the circumference of the LEP ring. After correction for this orbit lengthening, the remaining RMS spread of the energy calibrations is about 3.4 MeV for Peak-2 and 1.7 MeV for Peak+2. There are indications that this change in the orbit circumference is correlated with rainfall during the second half of the year 1993. The remaining fluctuations of the energy calibrations are not understood at present, but they might be due to magnetic fields.

The understanding of the LEP beam energy has been improved substantially in 1993, but a few problems remain. The sudden energy jumps during the temperature experiment are not explained. The behavior of the NMR probe reference is not yet well understood. The positron energy has not been measured accurately. For these reasons, the studies will be pursued. To fasten the energy calibration procedure and to improve its accuracy, experiments are planned to obtain transverse polarization with colliding beams. This would allow a monitoring of the beam energies during certain parts of the physics fills.

9 Acknowledgments

We would like to thank the LEP operations team for their excellent work in the difficult task of getting the last percent of polarization out of LEP. We are deeply indebted to F. Bordry and R. Billen for the excellent performance of the LEP data logging system. We would like to thank Prof. P. Melchior of the Royal Observatory in Bruxelles for the code to evaluate the tides. We thank CERN, the Max-Planck-Institut für Physik, München and the Ecole Polytechnique, Paris for their support.

References

- [1] L. Knudsen et al., Phys. Lett. B270 (1991) 97.
- [2] L. Arnaudon. et al., Phys. Lett. B284 (1992) 431.

- [3] M. Placidi et al., "Polarization Results and Future Perspectives", Proc. of the Third Workshop on LEP Performance, J. Poole Editor, CERN SL/93-19 (DI) (1993) 281.
- [4] The Working Group on LEP Energy and the LEP Collaborations ALEPH, DELPHI, L3 and OPAL, Phys. Lett. B 307 (1993) 187.
- [5] L. Arnaudon et al., "The energy Calibration of LEP in 1991", CERN-PPE/92-125 (1992).
- [6] M. Placidi and R. Rossmanith, Nucl. Instr. Meth. A274 (1989) 79.
- [7] B. Dehning, "Elektronen- und Positronen-Polarisation im LEP-Speicherring und Präzisionsbestimmung der Masse des Z-Teilchens", PhD thesis at the Ludwigs-Maximilians-Universität München, 1994, to be published.
- [8] R. Assmann et al., "Polarization Studies at LEP in 1993", CERN-SL/94-08 (AP) (1994).
- [9] M. Mayout and A. Verdier, "Survey and correction of LEP elements", Proc. of the Third Workshop on LEP Performance, J. Poole Editor, CERN SL/93-19 (DI) (1993) 147.
- [10] J. Borer, "BOM system hardware status", Proc. of the Third Workshop on LEP Performance, J. Poole Editor, CERN-SL/93-19 (DI) (1993) 219.
- [11] G. Vismara, "The new front-end Narrow-Band electronics for the LEP Beam Orbit Measurement system", Contribution to the 1994 European Particle Accelerator Conference, London, July 1994.
- [12] R. Assmann, "Transversale Strahlpolarisation und ihre Anwendung für Präzisionsmessungen bei LEP", PhD thesis at the Ludwigs-Maximilians-Universität München, 1994, to be published.
- [13] A. Blondel, "Compensation of Integer Spin Resonances Created by Experimental Solenoids", LEP Note 629 (1990).
- [14] V. Bargmann, L. Michel and V.L. Telegdi, Phys. Rev. Lett. 10 (1959) 435.
- [15] The Particle Data Group, Phys. Rev. D45, Part 2 (1992).
- [16] A.A. Sokolov and I.M. Ternov, Sov. Phys. Dokl. 8 (1964) 1203.
- [17] V. N. Baier and Y.F. Orlov, Sov. Phys. Dokl. 10 (1966) 1145.
- [18] A.A. Zholentz et al., Phys. Lett. 96B (1980) 214.
- [19] A.S. Artamonov et al., Phys. Lett. 118B (1982) 225.
- [20] Y.M. Shatunov and A.N. Skrinsky, Particle World, Vol. 1, No. 2 (1989) 35.
- [21] D.P. Barber et al., Phys. Lett. 135B (1984) 498.
- [22] W.W McKay et al., Phys. Rev. D29 (1984) 2483.
- [23] M. Froissart and R. Stora, Nucl. Instr. Meth. 7 (1960) 297.
- [24] J. Buon, "Interference Effects between Depolarization Resonances and Higher-Order Corrections to Perturbed Spin Motion in Synchrotrons and Storage Rings", LAL-RT 87-09.
- [25] J.P. Koutchouk, "Spin Tune Shifts due to Solenoids", CERN SL-Note/93-26 (AP) (1993).
- [26] R. Assmann and J.P. Koutchouk, "Spin Tune Shifts due to Optics Imperfections", CERN-SL/94-13 (AP) (1994).
- [27] I.A. Koop et al., "Investigation of the Spin Precession Tune Spread in the Storage Ring". Proc. 8th International Symposium on High Energy Spin Physics, Minneapolis, September 12-17, 1988, AIP Conf. Proc. No. 187, p. 1023.

- [28] Report of the working group on high luminosities at LEP, "High-Luminosity Options for LEP", J.M. Jowett Editor, CERN 91-02 (1991).
- [29] J. Jowett, "Effect of Pretzel Orbits on Energy Calibration", Proc. of the Third Workshop on LEP Performance, J. Poole Editor, CERN SL/93-19 (DI) (1993) 341.
- [30] M. Sands, "The Physics of Electron Storage Rings. An Introduction", SLAC-121 and UC-28 (1970).
- [31] H. Grote, C. Iselin, The MAD program V8.10, CERN-SL/90-13 Rev. 3 (AP).
- [32] G. Fischer and A. Hofmann, "Effects of tidal forces on the LEP energy", Proc. of the Second Workshop on LEP Performance, J. Poole Editor, CERN-SL/92-29 (DI) (1992).
- [33] L. Arnaudon et al., "Effects of Tidal Forces on the Beam Energy in LEP". Proc. of the 1993 Particle Accelerator Conference, May 1993, Washington.
- [34] P. Melchior, "The Tides of the Planet Earth", 2nd edition, Pergamon Press, 1983.
- [35] Program and input data from P. Melchior, International Center for Earth Tides, Bruxelles, Belgium.
- [36] L. Arnaudon et al., "Effects of Terrestrial Tides on the LEP Beam Energy", CERN-SL/94-07 (BI) (1994).
- [37] J. Wenninger, "Study of the LEP Beam Energy with Beam Orbits and Tunes". CERN-SL/94-14 (BI) (1994).
- [38] P. Collier, "Effect of QF-QD Compensation On LEP Beam Energy", CERN SL-MD Note 105 (1993).
- [39] J. Poole, "Effects of QF-QD Compensator", CERN SL-MD Note 131 (1994).
- [40] R. Bailey et al., "LEP Energy Calibration", Proc. of the 2nd European Particle Accelerator Conference, Nice, France (1990) and CERN SL/90-95.
- [41] H. Schmickler, "Measurements of the Central Frequency of LEP", CERN SL-MD Note 89 (1993).
- [42] M. Placidi and J. Pinfeld, Minutes of the 38th meeting of the LEP Energy Calibration Working Group, Oct. 1992.
- [43] L. Rolandi and M. Vandon, Minutes of the 50th meeting of the LEP Energy Calibration Working Group, Feb. 1993.
- [44] J. Billan et al., "Determination of the particle momentum in LEP from precise magnet measurements", Proc. of the 1991 Particle Accelerator Conference, San Francisco, CA (1991) and CERN-AT-MA-91-03.
- [45] K. Henrichsen, "Field Display and Flux-Loop Performance in 1992", Proc. of the Third Workshop on LEP Performance, J. Poole Editor, CERN-SL/93-19 (DI) (1993) 329.
- [46] J. Gascon, Minutes of the 44th meeting of the LEP Energy Calibration Working Group, Dec. 1993.
- [47] R. Forest, "Main Bend Power Converter Current Stability", Proc. of the Third Workshop on LEP Performance, J. Poole Editor, CERN-SL/93-19 (DI) (1993) 325.
- [48] P. Renton, Minutes of the 46th meeting of the LEP Energy Calibration Working Group, Dec. 1993.
- [49] A. Beuret et al., Minutes of the 39th meeting of the LEP Energy Calibration Working Group, Oct. 1993.

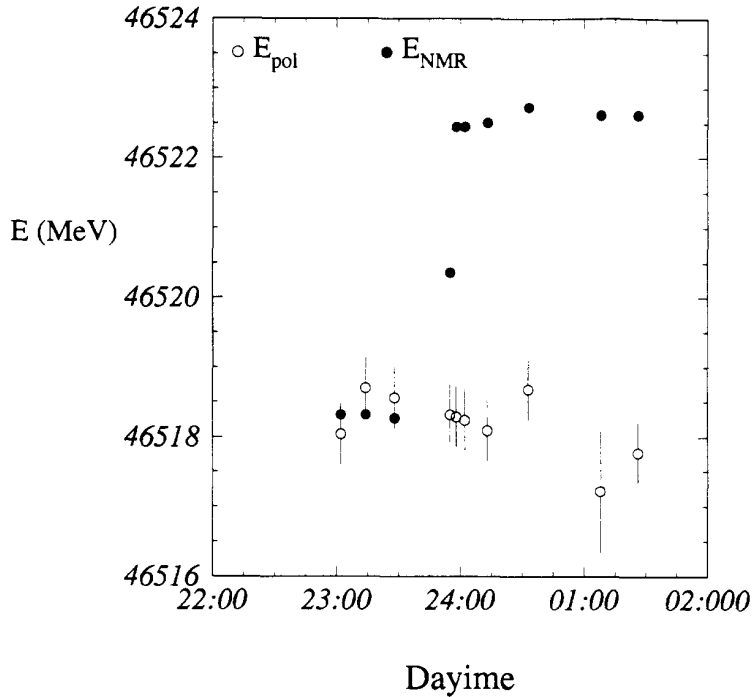


Figure 23: Evolution of E_{pol} , the energy measured by resonant depolarization, and E_{NMR} during the “current spike experiment”. Starting 23:55 current spikes were induced on the main bending magnets current supply. Only the NMR showed a 4 MeV energy jump. The errors indicated for E_{pol} correspond to the limits of the frequency scans. E_{pol} has been corrected for tide effects.

A Appendix : Magnetic field reference

To improve the understanding of the time evolution of the energy during fills or for a whole running period, it is useful to be able to track relative changes of the LEP bending field (~ 950 Tm at 45 GeV). Two devices are available for this task :

- The DCCTs (Direct Current Current Transformers [47]) measure the current flowing through all the main bending magnets with a resolution of ~ 0.5 MeV.
- A NMR probe measures the field inside a reference magnet with a resolution of ~ 0.1 MeV. The reference magnet is connected in series with the main bending magnets.

The reading of the DCCTs was very stable in 1993 for each energy point [48], but it cannot account for hysteresis effects in the magnets. Only tiny current variations were observed inside fills and over time. The current setting of the LEP main bending magnets was extremely stable during 1993.

A better tracking of the bending field could be provided by the NMR probe. This probe measures the field of the reference magnet and takes into account the magnetic hysteresis. The analysis of the NMR data shows sudden “jumps” of up to +5 MeV between two consecutive the readings. All jumps correspond to an increase of the field. In 1993, such jumps were observed in 5 to 10% of all physics fills. As a possible explanation, it was shown that such jumps can be produced by current spikes on the power supply of the main bending magnets [49]. To determine if these jumps correspond also to a real field increase for the LEP bending magnets, a specific experiment was performed where current spikes were deliberately applied on the main power supply. The NMR readings showed a clear +4 MeV jump, but no effect was observed on the beam energy measurement from resonant depolarization (figure 23). This behavior might

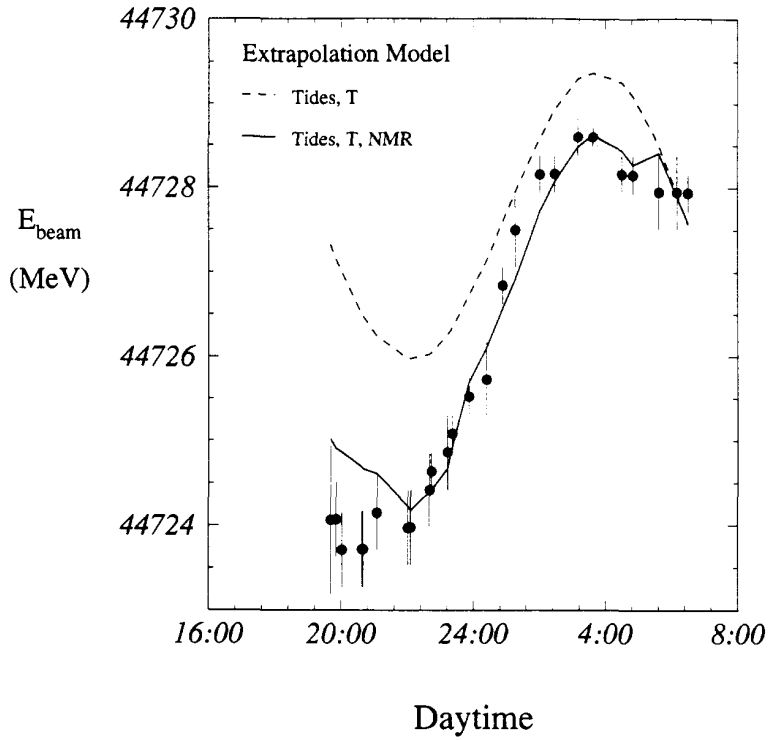


Figure 24: Extrapolation of the beam energy back in time, starting from the last calibrations in LEP fill 1849. Two extrapolation models are compared with (full line) and without NMR (dashed line). The data points favor an extrapolation including the NMR.

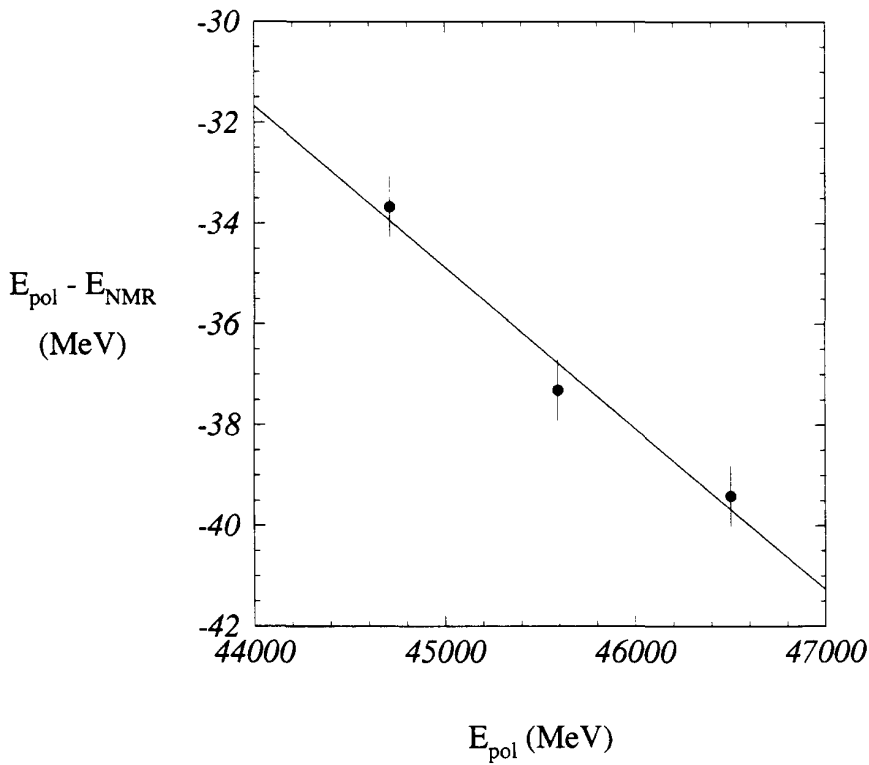


Figure 25: Energy difference between the energy measured by resonant depolarization and by the NMR probe in the reference magnet as a function of the beam energy.

be due to a shielding effect of the beam pipe, but it cannot explain why in a previous test, the beams were lost after a spike with an amplitude of ~ 20 MeV was applied with the same method. Unfortunately, no spontaneous jump was observed during energy calibrations and it is still not clear if these correspond to real field variations. For the analysis of the calibration data, jumps larger than 1 MeV between two consecutive readings have been corrected out.

The NMR displays another characteristic behavior. During fills, it almost always shows drifts towards higher fields. The drifts can reach a few MeV after 12 hours. We have indications that these slow drifts correspond to true field changes. This is demonstrated in figure 24 where the beam energy is extrapolated backward in time starting from the last calibration in LEP fill 1849. Without the use of the NMR, there is a 2.5 MeV discrepancy between the measured and the extrapolated beam energy at the beginning of the experiment.

These observations cast a doubt on whether the NMR can be used to track the bending field during LEP runs. The resulting systematic error on the Z mass and width can be estimated by comparing the results obtained using this reference or only the dipole current readings.

The LEP reference magnet has been calibrated with the total dipole field of all the normal LEP bending magnets at the time of the installation in the tunnel. Because the tunnel magnets are aging, their average field calibration varies. As a consequence the difference between the energy measured by depolarization and by the NMR probe depends on the energy, as can be seen in figures 16 and 20. We define this as the non-linearity of the reference magnet. The non-linearity can be measured with successive energy calibrations inside the same fill using a beam energy ramp. The result of such an experiment was (figure 25) :

$$(27) \quad \alpha_{nl} = \frac{(E_{pol} - E_{NMR})^{P+2} - (E_{pol} - E_{NMR})^{P-2}}{E_{pol}^{P+2} - E_{pol}^{P-2}} = (-3.20 \pm 0.47) \times 10^{-3}$$

From the average difference between energy calibrations at Peak-2 and Peak+2 (table 10), a lower value of $\alpha_{nl} = (-1.3 \pm 0.6) \times 10^{-3}$ is obtained. But figure 20 seems to indicate that the non-linearity might have varied with time or that other unknown causes for energy variations perturb the measurements of the non-linearity.

B Appendix : Calibrated fill energies

The following three tables contain the list of energies for all calibrated LEP fills. The energies E_{pol} are corrected to the reference values of the different parameters according to table 9. The RMS error σ_E includes the contributions from the errors on the correction coefficients as indicated in table 9. σ_E is dominated by the extrapolation errors. The average magnet temperature T_{mag} and the setting of the quadrupole compensation loop I_{Qfd} are also indicated. Fills marked with a * correspond to LEP Machine Development (MD) calibrations or special experiments which are not always performed with the same LEP settings than calibrations at the end of physics fills.

Fill	Date	E_{pol} (MeV)	σ_E (MeV)	T_{mag} (deg)	I_{Qfd} (A)
1579*	02-06-93	44720.6	1.6	23.16	—
1589*	04-06-93	44723.5	1.2	23.01	—
1616*	14-06-93	44712.2	0.9	23.29	—
1617*	14-06-93	44713.5	0.9	23.25	—
1636*	20-06-93	44717.8	1.4	22.84	—
1637*	21-06-93	44712.3	1.2	23.18	—
1660	05-07-93	44717.3	0.4	23.85	32.
1674	12-07-93	44718.9	0.6	23.87	32.
1694	19-07-93	44720.4	1.6	24.03	-40.
1734*	04-08-93	44709.0	0.6	23.56	32.
1745	12-08-93	44709.8	1.5	23.90	-40.
1764	21-08-93	44708.2	1.5	24.07	-40.
1771*	28-08-93	44709.6	1.4	22.79	32.
1772*	29-08-93	44709.0	1.2	22.98	32.
		44711.3	1.0	23.23	32.
		44713.0	0.7	23.44	32.
1794	04-09-93	44717.2	1.5	23.75	-40.
1837	05-10-93	44722.2	0.9	23.55	1.
1849	11-10-93	44726.6	0.5	23.73	32.
1861	16-10-93	44729.4	0.5	23.76	32.
1892	29-10-93	44722.8	0.4	23.83	32.
1927	09-11-93	44715.7	0.6	23.60	32.
1928	10-11-93	44715.8	0.5	23.75	32.
1937	15-11-93	44710.9	0.8	23.76	-1.

Table 11: Energies for all Peak-2 fills calibrated in 1993. In fill 1745, the beam energy was ramped from Peak-2 to Peak and Peak+2. For fill 1772 (the third experiment on the temperature coefficient) the 3 average energies before and after each energy jump are shown. For the first six fills, I_{Qfd} was not monitored.

Fill	Date	E_{pol} (MeV)	σ_E (MeV)	T_{mag} (deg)	I_{Qfd} (A)
1745*	04-08-93	45594.2	1.5	23.91	-41.
1935	14-11-93	45593.8	0.8	23.79	0.

Table 12: Energies for the 2 Peak fills calibrated in 1993. In fill 1745, the beam energy was ramped from Peak-2 to Peak and Peak+2.

Fill	Date	E_{pol} (MeV)	σ_E (MeV)	T_{mag} (deg)	I_{Qfd} (A)
1658	03-07-93	46512.1	0.4	23.81	33.
1672	10-07-93	46510.4	0.4	24.01	33.
1698	23-07-93	46510.4	1.5	24.14	-41.
1717	30-07-93	46509.3	1.5	24.21	-41.
1745*	04-08-93	46502.2	1.5	23.92	-41.
1761	18-08-93	46504.5	1.5	24.23	-41.
1811	12-09-93	46506.2	1.5	24.00	-41.
1845	10-10-93	46509.6	0.4	23.73	33.
1876	21-10-93	46515.4	0.5	23.84	33.
1888	26-10-93	46518.5	0.4	23.86	33.
1891	28-10-93	46514.6	0.4	23.90	33.
1930	11-11-93	46505.4	0.9	23.90	0.

Table 13: Energies for all Peak+2 fills calibrated in 1993. In fill 1745, the beam energy was ramped from Peak-2 to Peak and Peak+2.

